Copernicus Marine Service

QUALITY INFORMATION DOCUMENT

Mediterranean Sea Production Centre
MEDSEA_ANALYSISFORECAST_PHY_006_013

Issue: 2.3

Contributors: A.C. Goglio, E. Clementi, A. Grandi, A. Mariani, M.Giurato, A. Aydogdu

Approval date by the Copernicus Marine Service product quality coordination team:

CHANGE RECORD

When the quality of the products changes, the QuID is updated, and a row is added to this table. The third column specifies which sections or sub-sections have been updated. The fourth column should mention the version of the product to which the change applies.

Issue	Date	§	Description of Change	Author	Validated By
1.0	25-09-2017	All	Release of EAS2 version of the Med-Physics analysis and forecast product at 1/24° resolution	E. Clementi, A. Grandi, P. DiPietro, J. Pistoia, D. Delrosso, G. Mattia	E. Clementi (Med-MFC Deputy)
1.1	18-01-2018	All	Release of EAS3 version of the Med-Physics analysis and forecast product at 1/24° resolution	E. Clementi, A. Grandi, P. DiPietro, J. Pistoia, D. Delrosso, G. Mattia	E. Clementi (Med-MFC Deputy)
1.2	28-01-2019	All	Release of EAS4 version of the Med-Physics analysis and forecast product at 1/24° resolution	E. Clementi, A. Grandi, R. Escudier, V. Lyubartsev	E. Clementi (Med-MFC Deputy)
1.3	06-12-2019	All	Release of EAS5 version of the Med-Physics analysis and forecast product at 1/24° resolution	E. Clementi, A. Grandi, V. Lyubartsev	E. Clementi (Med-MFC Deputy)
1.4	10-09-2020	II.1 II.2 II.3 V	Use of higher resolution ECMWF atmospheric forcing	E. Clementi, A. Grandi, J. Pistoia	E. Clementi (Med-MFC Deputy)
2.0	15-01-2021	All	Updated document for the new product: modeling system including tides	E. Clementi, A. Grandi, A.C. Goglio, A. Aydogdu, J. Pistoia, V. Lyubartsev	E. Clementi (Med-MFC Deputy)
2.1	10-09-2021	II, IV, V	Updated document for new upstream river data	E. Clementi, A. Grandi, A.C. Goglio	E. Clementi (Med-MFC Deputy)
2.2	01-12-2021	IV, V	Updated document for SST satellite upstream data change and delivery of updated timeseries	E. Clementi	E. Clementi (Med-MFC Deputy)
2.2.1	23-09-2022	III. 4, V	Updated document for upstream data change: SLA Sentinel-6A assimilation	E. Clementi, A. Aydogdu, A. Grandi, A.C. Goglio	E. Clementi (Med-MFC Deputy)

Issue	Date	§	Description of Change	Author	Validated By
2.3	02-09-2022	All	Model and data assimilation improvements	A.C. Goglio, A. Grandi, E. Clementi, A. Aydogdu, A. Mariani	E. Clementi (Med-MFC Deputy)

TABLE OF CONTENTS

I EXECUTIVE SUMMARY

I.1 Products covered by this document

The product covered by this document is the MEDSEA_ANALYSISFORECAST_PHY_006_013: the analysis and forecast nominal product of the physical component of the Mediterranean Sea with 1/24° (~4.5 km) horizontal resolution and 141 vertical levels.

The variables produced are:

- 3D daily, hourly and monthly mean fields of: Potential Temperature, Salinity, Zonal, Meridional and Vertical Velocity
- 2D daily, hourly and monthly mean fields of: Sea Surface Height, De-tided Sea Surface Height, Sea Surface Zonal and Meridional Velocity, Mixed Layer Depth, Seabed Temperature (temperature of the deepest layer or level)
- 15 minutes instantaneous fields of: Sea Surface Height, Se Surface Zonal and Meridional Velocity

Product reference:

Clementi, E., Aydogdu, A., Goglio, A. C., Pistoia, J., Drudi, M., Grandi, A., Mariani, A., Lecci, R., Cretí, S., Coppini, G., Masina, S., & Pinardi, N. (2022). Mediterranean Sea Physical Analysis and Forecast (Copernicus Marine Service MED-Physics, EAS7 system) (Version 1) [Data set]. Copernicus Marine Service.
https://doi.org/10.25423/cmcc/medsea_analysisforecast_phy_006_013_eas7

I.2 Summary of the results

The quality of the MEDSEA_ANALYSISFORECAST_PHY_006_013 analysis and forecast product provided by the EAS7 modelling system, is assessed over 2 years period from 01/01/2020 to 31/12/2021 by means of temperature, salinity, sea level anomaly, sea surface height, currents, seabed temperature and mixed layer depth using independent (for surface currents and sea surface height), quasi-independent satellite and in-situ observations, climatological datasets as well as the inter-comparison with the previous version of the MEDSEA_ANALYSISFORECAST_PHY_006_013 product timeseries corresponding to the EAS7 modelling system.

The main results of the MEDSEA_ANALYSISFORECAST_PHY_006_013 quality assessment are summarized below:

Sea Surface Height: the EAS7 system presents a better accuracy in terms of sea surface height representation with respect to the previous version. The quality of the predicted SLA has been assessed by considering the RMS differences between the model daily outputs and the satellite along track observations, which is in average 3.0 cm. The new system presents a decreased error with respect to the previous one: 3.4 cm, the values are evaluated on the two years period 2020-2021. Moreover, the harmonic analysis shows that the model has a high skill in representing tidal amplitudes and phases of all the considered tidal constituents, with larger error for the higher tidal amplitudes.

Temperature: the temperature is accurate with an error below 0.88°C when compared to vertical in-situ observations per single vertical layer (Table 1), and 0.81°C when SST values are compared to satellite L4 dataset (Table 2) per each basin subregion (Figure 1). The accuracy of the temperature along the water column presents higher RMS differences at first layers, which decreases below 60 m. Considering the

SST, the RMS differences with respect to satellite observations vary in different subbasins, ranging from 0.51°C to 0.83°C. The product usually shows a warm SST bias.

Salinity: the salinity per single vertical layer is accurate with RMSD values lower than 0.19 PSU (Table **3**). The error is higher in the upper layers and decreases significantly below 150 m.

Currents: Surface currents RMSD and bias are evaluated against moored buoys. Due to the reduced number of observations, mainly located in coastal areas of the west side of the basin, the statistical relevance of currents performance is poor. In addition to the surface currents validation assessment, a derived validation assessment is provided in terms of transport at Straits including the net, eastward and westward transport through the Strait of Gibraltar showing a good agreement with literature values.

Bottom temperature: the bottom temperature of EAS7 system has been compared to SeaDataNet monthly climatology showing a good skill in representing the seasonal variability of the temperature at deepest level and a general overestimation with respect to the climatological dataset. The spatial pattern of the seabed temperature is correctly represented by the system.

Mixed Layer Depth: the MLD in the EAS7 system has been compared to climatological estimates from literature (Houpert at al., 2015) showing that the model is able to correctly represent the depth of the mixed layer with spatial and seasonal differences. In general, it can be noticed that the main differences could arise due to the low resolution of the climatological dataset which, in addition, do not covers the whole domain of the Mediterranean Sea.

I.3 Estimated Accuracy Numbers

Estimated Accuracy Numbers (EANs), namely the mean and the RMS of the difference between the model and in-situ or satellite reference observations, are provided in the following table.

EAN are computed for:

- Temperature;
- Salinity;
- Sea Surface Temperature (SST);
- Sea Level Anomaly (SLA).

The observations used are:

- vertical profiles of temperature and salinity from Argo floats:
  INSITU_MED_TS_NRT_OBSERVATIONS_013_035
- SST satellite data from Copernicus Marine SST-TAC product:

  SST_MED_SST_L4_NRT_OBSERVATIONS_010_004,
  SST_MED_SST_L3S_NRT_OBSERVATIONS_010_012
- Satellite Sea Level along track data from Copernicus Marine SeaLevel-TAC product:

  SEALEVEL_EUR_PHY_L3_REP_OBSERVATIONS_008_061

The EANs are evaluated for the EAS7 system over a two-years period, from January 2020 to December 2021, and are computed for the whole Mediterranean Sea and its 16 sub-regions depicted in Figure 1: (1) Alboran Sea, (2) South West Med 1 (western part), (3) North West Med, (4) South West Med 2 (eastern part), (5) Tyrrhenian Sea 2 (southern part), (6) Tyrrhenian Sea 1 (northern part), (7) Ionian Sea

1 (western part), (8) Ionian Sea 2 (south-eastern part), (9) Ionian Sea 2 (north-eastern part), (10) Adriatic Sea 2 (southern part), (11) Adriatic Sea 1 (northern part), (12) Levantine Sea 1 (western part), (13) Aegean Sea, (14) Levantine Sea 2 (central-northern part), (15) Levantine Sea 3 (central southern part), (16) Levantine Sea 4 (eastern part).

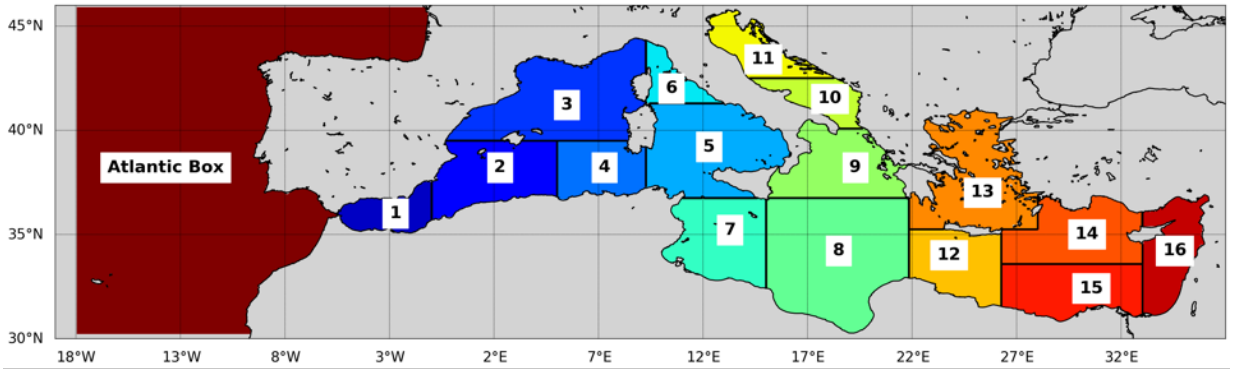

Figure 1. The Mediterranean Sea sub-regions subdivision for validation metrics

The EANs of temperature and salinity are then evaluated at 9 different layers: 0-10, 10-30, 30-60, 60-100, 100-150, 150-300, 300-600, 600-1000, 1000-2000 meters in order to better verify the model ability to represent the vertical structure of the temperature and salinity fields.

In the following Tables (Table 1, Table 2, Table 3 and Table 4) the EANs corresponding to Mean (Observations minus Model) and RMSD for the EAS7 system are presented together with the number of available insitu observations used for the computation of the values. In a few cases a lower model skill in terms of EANs can be attributed to the lower availability of measurements in the specific layer/area.

Temperature EANs	**EAS7 system**		
Layer [m]	**Mean [°C] (Obs-Model)**	**RMSD [°C]**	**OBS Num [#]**
0-10	0.00	0.59	67 K
10-30	0.03	0.88	162 K
30-60	-0.06	0.82	243 K
60-100	-0.03	0.47	326 K
100-150	-0.01	0.28	335 K
150-300	0.01	0.21	873 K
300-600	0.00	0.18	1139 K
600-1000	-0.01	0.09	944 K
1000-2000	-0.02	0.05	805 K

Table 1: The EANs of temperature at different vertical layers evaluated for the EAS7 system for the two-years period 2020-2021. The number of available insitu observations per layer in the two years period 2020-2021 is provided in the third column.

SST EANs	EAS7 system		
REGION	Mean [°C] (Obs-Model)	RMSD [°C]	OBS Num [#]
MED SEA	-0.10	0.61	46.2 M
REGION 1	0.32	0.83	1.2 M
REGION 2	0.03	0.51	3.1 M
REGION 3	-0.01	0.61	5.0 M
REGION 4	-0.13	0.64	2.0 M
REGION 5	-0.08	0.53	4.3 M
REGION 6	-0.16	0.52	0.9 M
REGION 7	-0.18	0.52	3.1 M
REGION 8	-0.21	0.75	6.9 M
REGION 9	-0.07	0.58	2.8 M
REGION 10	-0.14	0.54	1.2 M
REGION 11	0.03	0.62	1.3 M
REGION 12	-0.14	0.53	2.5 M
REGION 13	0.02	0.58	3.6 M
REGION 14	-0.12	0.56	3.1 M
REGION 15	-0.20	0.64	3.0 M
REGION 16	-0.24	0.56	2.2 M

Table 2: The EANs of Sea Surface Temperature evaluated for the EAS7 system for the two-years period 2020-2021 for the Mediterranean Sea and 16 regions (see Figure 1). The number of available satellite observations per subregion in the two-years period 2020-2021 is provided in the third column.

Salinity EANs	EAS7 system		
Layer [m]	Mean [PSU] (Obs-Model)	RMSD [PSU]	OBS Num [#]
0-10	-0.02	0.19	67 K
10-30	-0.01	0.19	164 K
30-60	0.00	0.18	245 K
60-100	0.01	0.14	326 K
100-150	0.01	0.11	335 K
150-300	0.00	0.07	873 K
300-600	0.00	0.04	1139 K
600-1000	0.00	0.02	944 K
1000-2000	0.00	0.02	805 K

Table 3: The EANs of salinity at different vertical layers evaluated for the EAS7 system for the two-years period 2020-2021. . The number of available insitu observations per subregion in the two-years period 2020-2021 is provided in the third column.

SLA EANs	EAS7 system	
REGION	RMSD [cm]	OBS Num [#]
MED SEA	3.2	713 K
REGION 1	4.5	19 K
REGION 2	3.2	49 K
REGION 3	2.9	81 K
REGION 4	3.9	34 K
REGION 5	3.4	69 K
REGION 6	3.1	14 K
REGION 7	3.6	51 K
REGION 8	3.5	113 K
REGION 9	2.5	40 K
REGION 10	2.5	17 K
REGION 11	2.5	18 K
REGION 12	2.8	37 K
REGION 13	3.2	38 K
REGION 14	2.7	50 K
REGION 15	3.2	46 K
REGION 16	2.8	38 K

Table 4: The EANs of Sea Level Anomaly evaluated for the EAS7 system for the two-years period 2020-2021 for the Mediterranean Sea and the 16 sub-regions (see Figure 1). The number of available satellite observations per subregion in the two-years period 2020-2021 is provided in the third column.

The metrics of Table 1 and Table 2 give indications about the accuracy of MEDSEA_ANALYSISFORECAST_PHY_006_013 temperature variable along the water column and at the surface for the Mediterranean Sea and 16 sub-regions. The values for all the vertical levels are computed using Argo profiles while the SST is evaluated by comparison with respect to satellite observations. The temperature RMSD and MEAN values are higher at the first levels and decrease significantly below the fourth layer, which correspond to 60 meters depth. The RMSD is always lower than 0.88°C along the water column, while it ranges between 0.51°C and 0.83°C for the SST.

The statistics listed in Table 3 give indications about the accuracy of the MEDSEA_ANALYSISFORECAST_PHY_006_013 salinity field. The values for all the levels are computed using Argo profiles. The system presents a RMSD always lower than 0.19 PSU with higher error at the surface which decreases below 150 meters.

The metrics shown in Table 4 define the accuracy of MEDSEA_ANALYSISFORECAST_PHY_006_013 sea level anomaly. The statistics are computed along the satellite tracks. The new system presents an overall RMS difference of 3.2 cm in the whole basin, while it ranges between 2.5 cm and 4.5 cm in the different regions.

II PRODUCTION SYSTEM DESCRIPTION

Production centre name: CMCC

Production system name: Analysis and Forecast Med-Physics EAS7 system

Copernicus Marine Product name: MEDSEA_ANALYSISFORECAST_PHY_006_013

External product: Temperature (3D), Salinity (3D), Meridional and Zonal Currents (3D), Vertical Velocity (3D), Sea Surface Height (2D), de-tided Sea Surface Height (2D), Mixed Layer Depth (2D), Seabed Temperature (2D)

Frequency of model output: daily (24-hrs) averages, hourly (1-hr) averages, monthly averages, 15 min instantaneous fields

Geographical coverage: -17.2917°W → 36.29167°E; 30.1875°N → 45.97917°N (Bay of Biscay and Black Sea are excluded)

Horizontal resolution: 1/24°

Vertical coverage: From surface to 5754 m (141 vertical unevenly spaced levels).

Length of forecast: 10 days for the daily mean fields, 5 days for the hourly mean fields.

Frequency of forecast release: Daily.

Analyses: Yes.

Hindcast: Yes.

Frequency of analysis release: Weekly on Tuesday.

Frequency of hindcast release: Daily.

The analyses and forecasts physical product of the Med-MFC is produced with two different cycles: a daily cycle for the production of forecast, and a weekly cycle for the production of analysis.

The daily cycle is done each day (J), for the next 10 days. The forecast is initialized by a hindcast every day except Tuesday, when the analysis is used instead of the hindcast. Every day the product is updated with a hindcast for day J-1 and 10-day forecast.

The weekly cycle is done on Tuesday, for the previous 15 days. The assimilation cycle is daily (24hr) and is done in filter mode. Every Wednesday the product is updated with the analyses from day J-15 to day J-2, a hindcast for day J-1 and 10-day forecast.

The production chain is illustrated in Figure 2.

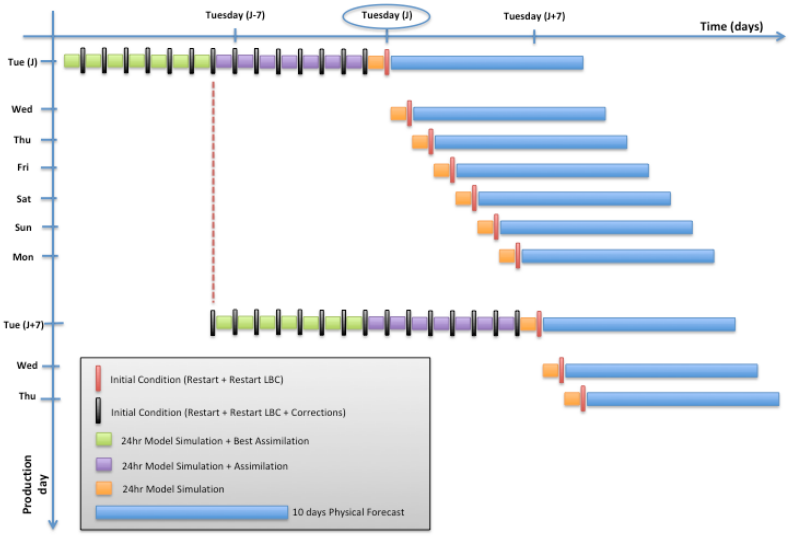

Figure 2: Scheme of the analysis and forecast Copernicus Marine Med-Physics processing chain.

The Med-Physics system run is composed by several steps:

1. Upstream Data Acquisition, Pre-Processing and Control of: ECMWF atmospheric forcing (Numerical Weather Prediction), Satellite (SLA and SST) and in-situ (T and S) observations.
2. Forecast/Hindcast: NEMO-WW3 modelling system is run to produce one day of hindcast and a 10-day forecast.
3. Analysis/Hindcast (only on Tuesday): NEMO-WW3 modelling system is coupled with OceanVar, a 3DVar assimilation scheme, in order to produce the best estimation of the sea (i.e. analysis). The NEMO+WW3+OceanVar system is running for 15 days into the past in order to use the best available along track SLA products. The latest day of the 15 days of analysis, produces the initial condition for the 10-day forecast.
4. Post processing: the model output is processed in order to obtain the products for the Copernicus Marine Service catalogue.
5. Output Delivery.

II.1 Description of the Med-Physics EAS7 model system

The Mediterranean Forecasting System, MFS, (Pinardi et al., 2003, Pinardi and Coppini 2010, Tonani et al., 2014) is providing, since year 2000, analysis and short-term forecast of the main physical parameters in the Mediterranean Sea and it is the physical component of the Med-MFC called Med-**Physics**.

The analysis and forecast Med-**Physics** system at Copernicus Marine EAS7 is provided by means of a coupled hydrodynamic-wave model implemented over the whole Mediterranean basin and extended into the Atlantic Sea in order to better resolve the exchanges with the Atlantic Ocean at the Strait of Gibraltar. The model horizontal grid resolution is 1/24˚ (ca. 4 km) and has 141 unevenly spaced vertical levels.

The hydrodynamics are supplied by the Nucleous for European Modelling of the Ocean (NEMO v3.6) while the wave component is provided by WaveWatch-III. The model solution is analysed and updated by OceanVar (an ocean 3DVar scheme) assimilating temperature and salinity vertical profiles and along track satellite sea level anomaly observations.

Circulation model component (NEMO)

The oceanic equations of motion of Med-Physics system are solved by an Ocean General Circulation Model (OGCM) based on NEMO (Nucleus for European Modelling of the Ocean) version 3.6 (Madec et al., 2019). The code is developed and maintained by the NEMO-consortium.

NEMO has been implemented in the Mediterranean at 1/24° x 1/24° horizontal resolution and 141 unevenly spaced vertical levels (Clementi et al., 2017a) with time step of 120 s. The model covers the whole Mediterranean Sea and also extends into the Atlantic in order to better resolve the exchanges with the Atlantic Ocean at the Strait of Gibraltar.

The NEMO code solves the primitive equations using the time-splitting technique that is the external gravity waves are explicitly resolved with non-linear free surface formulation and time-varying vertical z-star coordinates.

The advection scheme for active tracers, temperature and salinity, is a mixed up-stream/MUSCL (Monotonic Upwind Scheme for Conservation Laws; Van Leer, 1979), originally implemented by Estubier and Lévy (2000) and modified by Oddo et al. (2009). The vertical diffusion and viscosity terms are a function of the Richardson number as parameterized by Pacanowsky and Philander (1981).

The model interactively computes air-surface fluxes of momentum, mass, and heat. The bulk formulae implemented are described in Pettenuzzo et al. (2010) and are currently used in the Mediterranean operational system (Tonani et al., 2015). A detailed description of other specific features of the model implementation can be found in Oddo et al., (2009, 2014).

The vertical background viscosity and diffusivity values are set to 1.2e-6 [m^2/s] and 1.0e-7 [m^2/s] respectively, while the horizontal bilaplacian eddy diffusivity and viscosity are set respectively equal to -1.2e8 [m^4/s] and -2.0e8 [m^4/s]. A quadratic bottom drag coefficient with a logarithmic formulation has been used according to Maraldi et al. (2013) and the model uses vertical partial cells to fit the bottom depth shape.

Tidal waves have been included since the EAS6 system version, so that the tidal potential is computed across the domain for the 8 major constituents of the Mediterranean Sea: M2, S2, N2, K2, K1, O1, P1, Q1. In addition, tidal forcing is applied along the lateral boundaries in the Atlantic Ocean by means of tidal elevation estimated using FES2014 (Carrere et al., 2016) tidal model and tidal currents evaluated using TUGO (Toulouse Unstructured Grid Ocean model, ex-Mog2D, Lynch and Gray 1979). In order to improve the description of tides a Topographic Wave Drag parameterization (Shakespeare, 2020) and a Correction to the Bottom Friction coefficient (Borile, 2022) have been added.

The hydrodynamic model is nested in the Atlantic within the Global analysis and forecast system GLO-MFC daily data set (1/12° horizontal resolution, 50 vertical levels) that is interpolated onto the Med-Currents model grid. Details on the nesting technique and major impacts on the model results are in Oddo et al., (2009).

The model is forced by momentum, water and heat fluxes interactively computed by bulk formulae using the 1/10° horizontal-resolution operational analysis and forecast fields from the European Centre for Medium-Range Weather Forecasts (ECMWF) at highest available time frequency (1 hour for the first 3 days of forecast, 3 hours for the following 3 days of forecast and 6 hours for the last 4 days of forecast and for the analysis) and the model sea surface temperature (details of the air-sea physics are in Tonani et al., 2008). The water balance is computed as Evaporation minus Precipitation and Runoff. The evaporation is derived from the latent heat flux, precipitation is provided by ECMWF as daily averages, while the runoff of the 39 rivers implemented is provided by:

*) daily mean observed discharge for the Po river distributed by ARPAE (Regional Agency for Prevention, Environment and Energy of Emilia-Romagna, Italy) and available from the website: https://simc.arpae.it/dext3r/. The Po river discharge is measured at the closing point of the drainage basin in Pontelagoscuro.

*) monthly mean datasets for the remaining 38 rivers: the Global Runoff Data Centre dataset (Fekete et al., 1999) for the Ebro, Nile and Rhone rivers; the dataset from Raicich (1996) for: Vjosë, Seman rivers; the UNEP-MAP dataset (Implications of Climate Change for the Albanian Coast, Mediterranean Action Plan, MAP Technical Reports Series No.98., 1996) for the Buna/Bojana river; the PERSEUS dataset for the following 32 rivers: Piave, Tagliamento, Soca/Isonzo, Livenza, Brenta-Bacchiglione, Adige, Lika, Reno, Krka, Arno, Nerveta, Aude, Trebisjnica, Tevere/Tiber, Mati, Volturno, Shkumbini, Struma/Strymonas, Meric/Evros/Maritsa, Axios/Vadar, Arachtos, Pinios, Acheloos, Gediz, Buyuk Menderes, Kopru, Manavgat, Seyhan, Ceyhan, Gosku, Medjerda, Asi/Orontes.

Objective Analyses-Sea Surface Temperature (OA-SST) fields from CNR-ISA SST-TAC are used for the correction of surface heat fluxes with the relaxation constant of 110 $Wm^{-2}K^{-1}$ centered at midnight since the observed dataset corresponds to the foundation SST (~SST at midnight).

The Dardanelles Strait is implemented as a lateral open boundary condition by using GLO-MFC daily Analysis and Forecast product and daily climatology derived from a Marmara Sea box model (Maderich et al., 2015).

The topography is created starting from the GEBCO 30arc-second grid (http://www.gebco.net/data_and_products/gridded_bathymetry_data/gebco_30_second_grid/), filtered (using a Shapiro filter) and manually modified in critical areas such as: islands along the Eastern Adriatic coasts, Gibraltar and Messina straits, Atlantic box edge.

Wave model component (WW3)

The wave dynamic is solved by a Mediterranean implementation of the WaveWatch-III (WW3) code version 3.14 (Tolman, 2009). WaveWatch covers the same domain and follows the same horizontal discretization of the circulation model (1/24° x 1/24°) with a time step of 240 sec. The wave model uses 24 directional bins (15° directional resolution) and 30 frequency bins (ranging between 0.05 Hz and 0.7931 Hz) to represent the wave spectral distribution.

WW3 has been forced by the same 1/10° horizontal resolution ECMWF atmospheric forcing (the same used to force the hydrodynamic model). The wind speed is then modified by considering a stability parameter depending on the air-sea temperature difference according to Tolman (2002).

The wave model takes into consideration the surface currents for wave refraction but assumes no interactions with the ocean bottom. WW3 model solves the wave action balance equation that describes the evolution, in slowly varying depth domain and currents, of a 2D ocean wave spectrum where individual spectral component satisfies locally the linear wave theory. In the present application WW3 has been implemented following WAM cycle4 model physics (Gunther et al., 1993). Wind input and dissipation terms are based on Janssen's quasi-linear theory of wind-wave generation (Janssen, 1989, 1991). The dissipation term is based on Hasselmann (1974) whitecapping theory according to Komen et al. (1984). The non-linear wave-wave interaction is modelled using the Discrete Interaction Approximation (DIA, Hasselmann et al., 1985).

Model coupling (NEMO-WW3)

The coupling between the hydrodynamic model (NEMO) and the wave model (WW3) is achieved by an online hourly two-way coupling and consists in exchanging the following fields: NEMO sends to WW3 the air-sea temperature difference and the surface currents, while WW3 sends to NEMO the neutral drag coefficient used to evaluate the surface wind stress.

More details on the model coupling and on the impact of coupled system on both wave and circulation fields can be found in Clementi et al., (2017b).

Data assimilation scheme (OceanVar)

The data assimilation system is based on a 3D variational ocean data assimilation scheme, OceanVar, developed by Dobricic and Pinardi (2008) and later upgraded by Storto et al. (2015). The background error covariance matrices vary monthly at each grid point in the discretized domain of the Mediterranean Sea. EOFs have been calculated from a three-years long simulation (in the future EOFs will be updated using the new long-term reanalysis product). The observations that are assimilated are: along-track sea level anomaly (a satellite product including dynamical atmospheric correction and ocean tides is chosen, as specified in II.3) from CLS SEALEVEL-TAC, and in-situ vertical temperature and salinity profiles from VOS XBTs (Voluntary Observing Ship-eXpandable Bathythermograph) and ARGO floats. In-situ observational errors are estimated iteratively as described in Desroziers et al. (2005). The altimeter observation errors are assumed to be the same for all satellites and is 3 cm. The misfits with the observations (innovations) are computed with the First Guess at Appropriate Time (FGAT) technique.

II.2 New features of the Med-Physics EAS7 system

The main differences between the Copernicus Marine Med-Physics EAS6 and EAS7 systems are summarized in Table 5 and described hereafter.

	Copernicus Marine Med-Physics EAS7
Upgrades in the modelling system	Added a Topographic Wave Drag parameterization to describe the momentum dissipation by tides over rough topography below 500 m depth. Modified the bottom friction coefficient in order to update the value at each barotropic time-step. Removed the increased bottom friction at Gibraltar strait. Increased the lateral friction at Gibraltar Strait. Modified the area of enhanced lateral friction at Messina Strait.
Changes in Data Assimilation	New MDT for SLA assimilation. Ingestion of filtered SLA observations at 7 km. Assimilation of new available satellite observations (HY-2B, Sentinel-6A).
New variables in catalogue	Added new 3D var: daily and monthly vertical velocity.

Table 5: Differences between Med-Physics EAS7 system and the previous one (EAS6).

II.3 Upstream data and boundary condition of the NEMO-WW3-OceanVar system

The Copernicus Marine MED-Physics system uses the following upstream data:

1. Atmospheric forcing (including precipitation): NWP 6-h (1-h for the first 3 days of forecast, 3-h for the following 3 days of forecast), 0.10° horizontal-resolution operational analysis and forecast fields from the European Centre for Medium-Range Weather Forecasts (ECMWF) distributed by the Italian National Meteo Service (USAM/CNMA)
2. Runoff: ARPAE (Regional Agency for Prevention, Environment and Energy of Emilia-Romagna, Italy, https://simc.arpae.it/dext3r/) daily measurements for the Po river; Monthly climatologies derived from: Global Runoff Data Centre dataset (Fekete et al., 1999) for Ebro, Nile and Rhone, the dataset from Raicich (1996) for the Adriatic rivers Vjosë and Seman; the UNEP-MAP dataset (Implications of Climate Change for the Albanian Coast, Mediterranean Action Plan, MAP Technical Reports Series No.98., 1996) for the Buna/Bojana river; the PERSEUS project dataset for the new 32 rivers added.
3. Initial conditions of temperature and salinity at 1/1/2015 are the winter climatological fields from WOA13 V2 (World Ocean Atlas 2013 V2, https://www.nodc.noaa.gov/OC5/woa13/woa13data.html)
4. Lateral boundary conditions from Copernicus Marine Global Analysis and Forecast system: GLOBAL_ANALYSISFORECAST_PHY_001_024 at 1/12° horizontal resolution, 50 vertical levels.

5. Lateral boundary tidal signal: tidal elevation from FES2014 (Carrere et al., 2016) and tidal currents from TUGO (Toulouse Unstructured Grid Ocean model, ex-Mog2D, Lynch and Gray 1979).
6. Data assimilation:
    - Temperature and Salinity vertical profiles from Copernicus Marine INSITU TAC
        - INSITU_MED_NRT_OBSERVATIONS_013_035
    - Satellite along track Sea Level Anomaly from Copernicus Marine SL TAC:
        - SEALEVEL_EUR_PHY_L3_REP_OBSERVATIONS_008_061 (until Dec 2021)
        - SEALEVEL_EUR_PHY_L3_NRT_OBSERVATIONS_008_059 (from Jan 2022 to present)
    - Satellite SST from Copernicus Marine SST TAC (nudging):
        - SST_MED_SST_L4_NRT_OBSERVATIONS_010_004

III VALIDATION FRAMEWORK

In order to evaluate and assure the quality of the MEDSEA_ANALYSISFORECAST_PHY_006_013 product, an assimilation experiment has been performed using the system described in section II, which is going to be operational starting in November 2022, and covering 7 years from January 2015 to December 2021 (the period from January to December 2015 is considered as a spin-up and performed without assimilation).

In particular, the qualification task has been carried out over a two-years period, from January 2020 to December 2021, based on Class 1, Class2 and Class4 diagnostics.

The performance of the Med-Physics EAS7 new system has been assessed by using external products: quasi-independent satellite and in-situ observations have been used to assess the skill of temperature, salinity and sea level anomaly; independent fixed moorings have been used to qualify coastal currents; independent tide gauges have been used to perform the harmonic analysis, moreover, climatological datasets have been used to assess the quality of the seabed temperature and mixed layer depth.

Quasi-independent data are all the observations (Satellite SLA and SST and in situ vertical profiles of temperature and salinity from XBT and Argo) which are assimilated into the system. Diagnostic in terms of RMS of the misfits and/or bias are computed using the model fields before the ingestion of the observations and applying the increments.

The datasets of observations used for the qualification task are listed below in Table 6 presenting the lists of the independent and quasi-independent datasets with the corresponding product names.

QUASI-INDEPENDENT DATA	
TYPE	**COPERNICUS MARINE PRODUCT NAME**
ARGO, XBT	INSITU_MED_NRT_OBSERVATIONS_013_035
SLA	SEALEVEL_EUR_PHY_L3_REP_OBSERVATIONS_008_061 SEALEVEL_EUR_PHY_L3_NRT_OBSERVATIONS_008_059
SST	SST_MED_SST_L4_NRT_OBSERVATIONS_010_004
INDEPENDENT DATA	
TYPE	**PRODUCT NAME**
MOORINGS, Tide gauges	INSITU_MED_NRT_OBSERVATIONS_013_035 EMODnet Physics

Table 6: list of the quasi-independent and independent observations

In this section the results of the validation task are presented in terms of: Temperature (including SST), Sea Bottom Temperature, Salinity, Sea Level Anomaly, Sea Surface Height, Currents (also in terms of transport at straits), and Mixed Layer Depth.

The list of metrics used to provide an overall assessment of the product, to quantify the differences with the available observations is presented in Table 7.

Name	Description	Ocean parameter	Supporting reference dataset	Quantity
NRT evaluation of Med-MFC-Physics using semi-independent data: Estimate Accuracy Numbers				
T-<X-Y>m-D-CLASS4-PROF-RMSD-Jan2020-Dec2021	Temperature vertical profiles comparison with respect to Copernicus Marine INSITU TAC data at several layers for the Mediterranean basin.	Temperature	Argo floats from the Copernicus Marine INSITU TAC product: INSITU_MED_NRT_OBSERVATIONS_013_035	Time series of Temperature daily RMSs of the difference between insitu observations and system outputs averaged over the qualification testing period (Jan 2020-Dec 2021). This quantity is evaluated on the model analysis. The statistics are defined for all the Mediterranean Sea and are evaluated for several layers. Together with the time series, the time (2020-2021) average RMSD value is reported in tables.
T-<X-Y>m-D-CLASS4-PROF-BIAS-Jan2020-Dec2021	Temperature vertical profiles comparison with respect to Copernicus Marine INSITU TAC data at several layers for the Mediterranean basin.	Temperature	Argo floats from the Copernicus Marine INSITU TAC product: INSITU_MED_NRT_OBSERVATIONS_013_035	Time series of Temperature daily mean differences between insitu observations and system outputs averaged over the qualification testing period (Jan 2020-Dec 2021). This quantity is evaluated on the model analysis. The statistics are defined for all the Mediterranean Sea and are evaluated for several different layers. Together with the time series, the time (2020-2021) averaged BIAS value is reported in tables.
S-<X-Y>m-D-CLASS4-PROF-RMSD-Jan2020-Dec2021	Salinity vertical profiles comparison with respect to Copernicus Marine INSITU TAC data at several layers for the Mediterranean basin.	Salinity	Argo floats from the Copernicus Marine INSITU TAC product: INSITU_MED_NRT_OBSERVATIONS_013_035	Time series of Salinity daily RMSs of the difference between insitu observations and system outputs averaged over the qualification testing period (Jan 2020-Dec 2021). This quantity is evaluated on the model analysis. The statistics are defined for all the Mediterranean Sea and are evaluated for several different layers. Together with the time series, the time (22020-2021) averaged RMSD value is reported in tables.
S-<X-Y>m-D-CLASS4-PROF-BIAS-Jan2020-Dec2021	Salinity vertical profiles comparison with Copernicus Marine INSITU TAC data at several layers for the Mediterranean basin.	Salinity	Argo floats from the Copernicus Marine INSITU TAC product: INSITU_MED_NRT_OBSERVATIONS_013_035	Time series of Salinity daily mean differences between insitu observations and system outputs averaged over the qualification testing period (Jan 2020-Dec 2021). This quantity is evaluated on the model analysis. The statistics are defined for all the Mediterranean Sea and are evaluated for several layers. Together with the time series, the time (2020-2021) averaged BIAS value is reported in tables.

Table 7: List of metrics for Med-Physics evaluation using in-situ and satellite observations (continues in next pages).

Name	Description	Ocean parameter	Supporting reference dataset	Quantity
NRT evaluation of Med-MFC-Physics using semi-independent data: Estimate Accuracy Numbers				
SST-SURF-D-CLASS4-RAD-RMSD-Jan2020-Dec2021	Sea Surface Temperature comparison with respect to SST Copernicus Marine SST TAC L4 (satellite) data for the Mediterranean basin and selected sub-basins.	Sea Surface Temperature	SST satellite data from Copernicus Marine SST TAC L4 product: SST_MED_SST_L4_NRT_OBSERVATIONS_010_004	Time series of Sea surface temperature daily RMSs of the difference between atellite observations and system outputs averaged over the qualification testing period (Jan 2020-Dec 2021). This quantity is evaluated on the model analysis. The statistics are defined for all the Mediterranean Sea, 16 selected sub-basins and the Atlantic box. Together with the time series, the time (2020-2021) average RMSD value is reported in tables.
SST-SURF-D-CLASS4-RAD-BIAS-Jan2020-Dec2021	Sea Surface Temperature comparison with respect to SST Copernicus Marine SST TAC L4 (satellite) data for the Mediterranean basin and selected sub-basins.	Sea Surface Temperature	SST satellite data from Copernicus Marine SST TAC L4 product: SST_MED_SST_L4_NRT_OBSERVATIONS_010_004	Time series of Sea surface temperature daily mean differences between satellite observations and system outputs averaged over the qualification testing period (Jan 2020-Dec 2021). This quantity is evaluated on the model analysis. The statistics are defined for all the Mediterranean Sea, 16 selected sub-basins basins and the Atlantic box. Together with the time series, the time (2020-2021) average BIAS value is reported in tables.
NRT evaluation of Med-MFC-Physics using semi-independent data. Weekly comparison of misfits				
T-<X-Y>m-2W-CLASS4-ASSIM–PROF-RMSD-MED-Jan2020-Dec2021	Temperature vertical profiles comparison with assimilated Copernicus Marine INSITU TAC data at 5 specified depths.	Temperature	Argo floats, CTD and XBT from the Copernicus INSITU TAC products: INSITU_MED_NRT_OBSERVATIONS_013_035	Time series of weekly RMSs of temperature misfits (observation minus system outputs value transformed at the observation location and time). Together with the time series, the average value of weekly RMSs is evaluated over the qualification testing period (2020-2021). The statistics are defined for all the Mediterranean Sea and are evaluated at five different depths: 8, 30, 150, 300 and 600 m.
S-<X-Y>m-2W-CLASS4–ASSIM-PROF-RMSD-MED-Jan2020-Dec2021	Salinity vertical profiles comparison with assimilated Copernicus Marine INSITU TAC data at 5 specified depths.	Salinity	Argo floats from the Copernicus Marine INSITU TAC products: INSITU_MED_NRT_OBSERVATIONS_013_035	Time series of weekly RMSs of salinity misfits (observation minus system outputs value transformed at the observation location and time). Together with the time series, the average value of weekly RMSs is evaluated over the qualification testing period (2020-2021). The statistics are defined for all the Mediterranean Sea and are evaluated at five different depths: 8, 30, 150, 300 and 600 m.
SLA-SURF-2W-CLASS4-ASSIM-ALT-RMSD-MED-Jan2020-Dec2021	Sea level anomaly comparison with assimilated Copernicus Marine Sea Level TAC satellite along track data for the Mediterranean basin.	Sea Level Anomaly	Satellites (Jason3, CryoSat-2, Altika, Sentinel3A/B, HY-2A/2B) Sea Level along track data from Copernicus Marine Sea Level TAC product: SEALEVEL_EUR_PHY_L3_NRT_OBSERVATIONS_008_059	Time series of weekly RMSs of sea level anomaly misfits (observation minus system outputs value transformed at the observation location and time). Together with the time series, the average value of weekly RMSs is evaluated over the qualification testing period (2020-2021). The statistics are defined for all the Mediterranean Sea and are evaluated for the different assimilated satellites.

Name	Description	Ocean parameter	Supporting reference dataset	Quantity
NRT evaluation of Med-MFC-Physics using semi-independent data. Depth-Time Weekly comparison of misfits (Hovmoller diagrams)				
T-<X-Y>m-2W-CLASS4–PROF-RMSD-MED-Jan2020-Dec2021-HOV	Temperature depth-time comparison with assimilated Copernicus Marine INSITU TAC between 0 and 900m.	Temperature	Argo floats, CTD and XBT from the Copernicus Marine INSITU TAC products: INSITU_MED_NRT_OBSERVATIONS_013_035	Depth-Time (Hovmoller diagram) of two-weekly RMS temperature misfits (observation minus system outputs value transformed at the observation location and time) evaluated over the qualification testing period (2020-2021). The statistics are averaged over the whole Mediterranean Sea and are defined between 0 and 900m depth.
S-<X-Y>m-2W-CLASS4–PROF-RMSD-MED-Jan2020-Dec2021-HOV	Salinity depth-time comparison with assimilated Copernicus Marine INSITU TAC between 0 and 900m.	Salinity	Argo floats, CTD and XBT from the Copernicus Marine INSITU TAC products: INSITU_MED_NRT_OBSERVATIONS_013_035	Depth-Time (Hovmoller diagram) of monthly RMS salinity misfits (observation minus system outputs value transformed at the observation location and time) evaluated over the qualification testing period (2020-2021). The statistics are averaged over the whole Mediterranean Sea and are defined between 0 and 900m depth.
NRT evaluation of Med-MFC-Physics using semi-independent data. 2D MAPS of Yearly comparison of Estimate Accuracy Numbers				
T-<X-Y>m-2Y-CLASS4–PROF-RMSD-TS-Jan2020-Dec2021-2DMAP	Temperature comparison with respect to Copernicus Marine INSITU TAC data at several layers for the Mediterranean basin.	Temperature	Argo floats and XBT from the Copernicus Marine INSITU TAC products: INSITU_MED_NRT_OBSERVATIONS_013_035	2D MAPS of RMSD of temperature (observation minus system outputs value transformed at the observation location and time) averaged over the qualification testing period (2020-2021). The statistics are defined for all the Mediterranean Sea and are evaluated in several vertical layers: 0-10, 10-30, 30-60, 60-100, 100-150, 150-300, 300-600, 600-1000, 1000-2000 meters.
S-<X-Y>m-2Y-CLASS4–PROF-RMSD-TS-Jan2020-Dec2021-2DMAP	Salinity comparison with respect to Copernicus Marine INSITU TAC data at several layers for the Mediterranean basin.	Salinity	Argo floats from the Copernicus Marine INSITU TAC products: INSITU_MED_NRT_OBSERVATIONS_013_035	2D MAPS of RMSD of salinity (observation minus model value transformed at the observation location and time) averaged over the qualification testing period (2020-2021). The statistics are defined for all the Mediterranean Sea and are evaluated in several vertical layers: 0-10, 10-30, 30-60, 60-100, 100-150, 150-300, 300-600, 600-1000, 1000-2000 meters.
SLA-SURF-2Y-CLASS4–ALT-RMSD-TS-Jan2020-Dec2021-2DMAP	Sea Level Anomaly comparison with respect to Copernicus Marine INSITU TAC.	Sea Level	Satellites (Jason3, CryoSat-2, Altika, Sentinel3A/B, HY-2A/2B) Sea Level along track data: SEALEVEL_EUR_PHY_L3_REP_OBSERVATIONS_008_061 SEALEVEL_EUR_PHY_L3_NRT_OBSERVATIONS_008_059	2D MAPS of RMSD of Sea Level Anomaly (observation minus model value transformed at the observation location and time) averaged over the qualification testing period (2020-2021). The statistics are defined for all the Mediterranean Sea

Name	Description	Ocean parameter	Supporting reference dataset	Quantity
NRT evaluation of Med-MFC-Physics using independent data. Daily comparison with moorings				
UV-SURF-D-CLASS2-MOOR-RMSD-Jan2020-Dec2021	Surface currents comparison with Copernicus Marine INSITU TAC	Currents	Moored buoys from Copernicus Marine InSitu TAC products: INSITU_MED_NRT_OBSERVATIONS_013_035	Time series of daily sea surface currents of insitu observations and model outputs evaluated over the qualification testing period. Together with the time series, the average value of daily RMSs is evaluated over the qualification testing period. This quantity is evaluated on the model analysis.
UV-SURF-D-CLASS2-MOOR-BIAS-Jan2020-Dec2021	Surface currents comparison with Copernicus Marine INSITU TAC	Currents	Moored buoys from Copernicus Marine InSitu TAC products: INSITU_MED_NRT_OBSERVATIONS_013_035	Time series of daily sea surface currents of insitu observations and model outputs evaluated over the qualification testing period. Together with the time series, the average value of daily bias is evaluated over the qualification testing period. This quantity is evaluated on the model analysis.
NRT evaluation of Med-MFC-Physics using Climatological dataset				
MLD-D-CLASS1-CLIM-MEAN_M-MED	Mixed Layer Depth comparison with climatology from literature in the Mediterranean Sea	Mixed Layer Depth	Monthly climatology from literature (Houpert et al., 2015)	Comparison of climatological maps form model outputs computed over the two-years period 2020-2021 and a climatological dataset (Houpert at al., 2015)
SBT-D-CLASS4-CLIM-MEAN_M-MED	Bottom Temperature comparison with a climatological dataset in the Mediterranean Sea	Sea Bottom Temperature	SeaDataNet climatological datasets	Time series of mean (computed over the two-years period 2020-2021) monthly mean Sea Bottom Temperature from model outputs and SeaDataNetEAS4 climatologies. The time series are presented for the entire basin, for the area with topography < 500m and for the areas with topography < 1500m
SBT-D-CLASS1-CLIM-MEAN_M-MED	Bottom Temperature comparison with a climatological dataset in the Mediterranean Sea	Sea Bottom Temperature	SeaDataNet climatological datasets	Comparison of climatological maps form model outputs computed over the two-years period 2020-2021 and SeaDataNet climatologies for the area with topography < 1500m

Table 7: (continued) List of metrics for Med-**Physics** evaluation using in-situ and satellite observations.

III.1 Temperature

In the following Table 7 the values of the temperature Root Mean Square (RMS) of differences and bias computed comparing the analysis of MEDSEA_ANALYSISFORECAST_PHY_006_013 product with quasi-independent data assimilated by the system (ARGO) are synthesised. The accuracy of SST is instead provided thorough the 2-weekly mean of EANs computation with respect to the satellite values used for the relaxation of surface heat fluxes. The synthesis is based on two-years period (2020-2021) validation and provided at 5 depths (8, 30, 150, 300, 600 m) showing that the larger error is achieved at 30 m depth while below it is lower than 0.3°C.

Variables/estimated accuracy:	Metrics		Depth [m]	Observation
SEA SURFACE TEMPERATURE	**RMSD [°C]**	**BIAS [°C]**		
	0.6 ± 0.1	-0.1 ± 0.1	0	Satellite SST
TEMPERATURE	**RMS misfits [°C]**		**Depth [m]**	**Observation**
	0.6 ± 0.2		8	Argo
	0.8 ± 0.4		30	Argo
	0.22 ± 0.05		150	Argo
	0.17 ± 0.03		300	Argo
	0.11 ± 0.02		600	Argo

Table 7: Quasi-independent validation. Analysis evaluation based over the two-years period 2020-2021.

Figure 3 shows the time series of two-weekly RMS of temperature misfits at 5 depths (8, 30, 150, 300, 600 m), T-<X-Y>m-2W-CLASS4- ASSIM–PROF-RMSD-MED-Jan2020-Dec2021, for the Copernicus Marine Med-MFC-Physics EAS7 system; the values of the mean RMS difference are given in the legend of the figures; the number of observed profiles is represented in shaded coloured areas.

The temperature error is generally higher at depth around 30 m and has a better skill below 150 m. It presents a seasonal variability at first layers with higher values during warm seasons.

Monthly mean RMS of temperature misfits are represented in the following (Depth-Time) Hovmoller diagrams (Figure 4), T-<X-Y>m-2W-CLASS4–PROF-RMSD-MED-Jan2020-Dec2021-HOV, along the water column between surface and 900 m showing the vertical pattern of the error averaged in the whole Mediterranean Sea. The system presents higher errors during summer-autumn seasons in the thermocline, between 30-60 m depth.

In addition to basin averaged statistics, the following panels in Figure show the spatial pattern of the temperature RMSD per subregion and per vertical layer, computed over the entire qualification period (2020-2021) with respect to ARGO data, T-<X-Y>m-2Y-CLASS4–PROF-RMSD-TS-Jan2020-Dec2021-2DMAP. The top left panel shows the number of observations along the whole water column used for this analysis. The maps confirm that the largest discrepancy occurs between 10-60 meters. The largest differences are located in the south-Tyrrhenian and South-Ionian Seas.

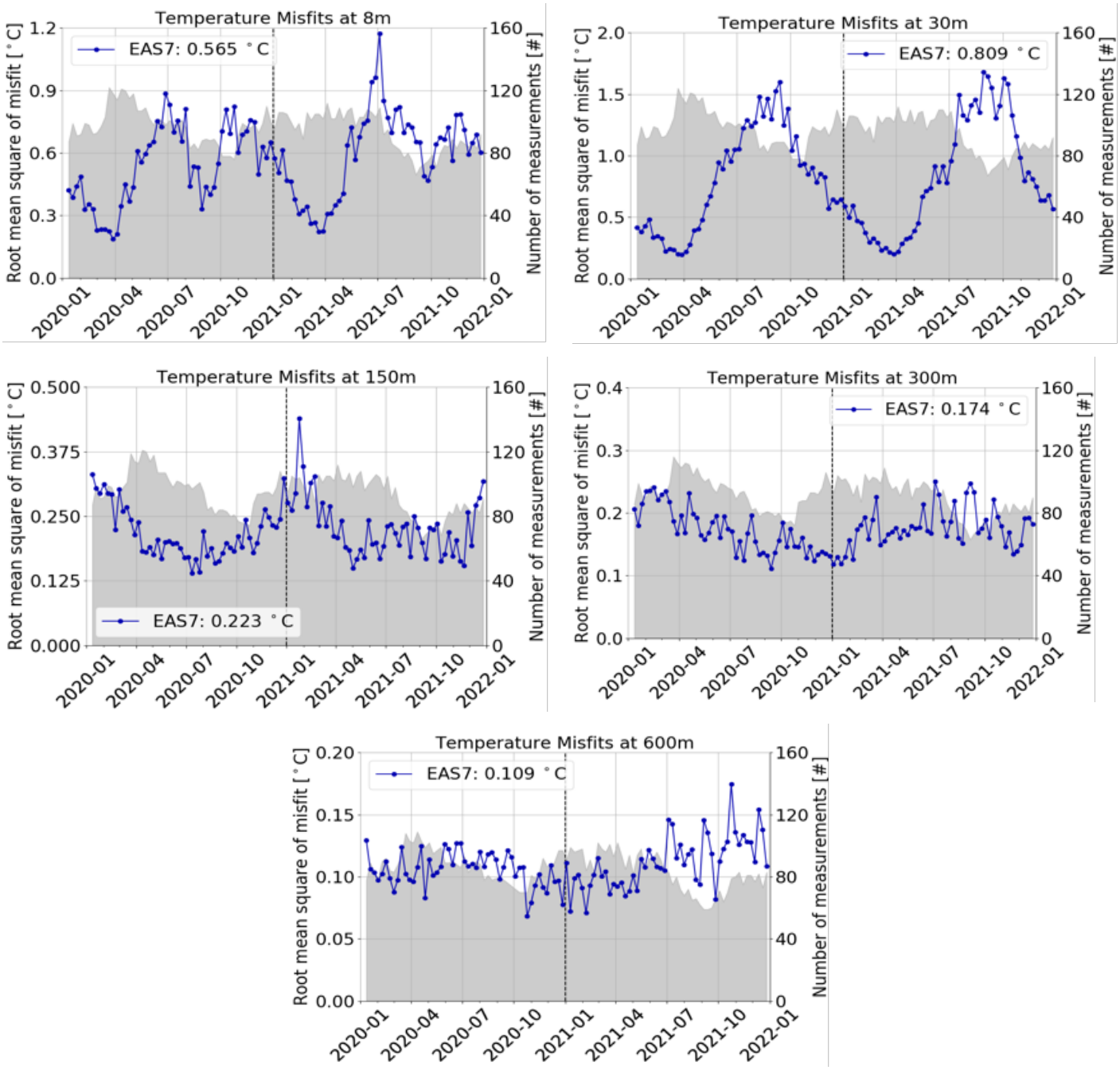

Figure 3: Time series of weekly RMS of temperature misfits (solid line) and number of observed profiles (shaded area) at 8, 30, 150, 300 and 600 meters (T-<X-Y>m-2W-CLASS4- ASSIM–PROF-RMSD-MED-Jan2020-Dec2021).

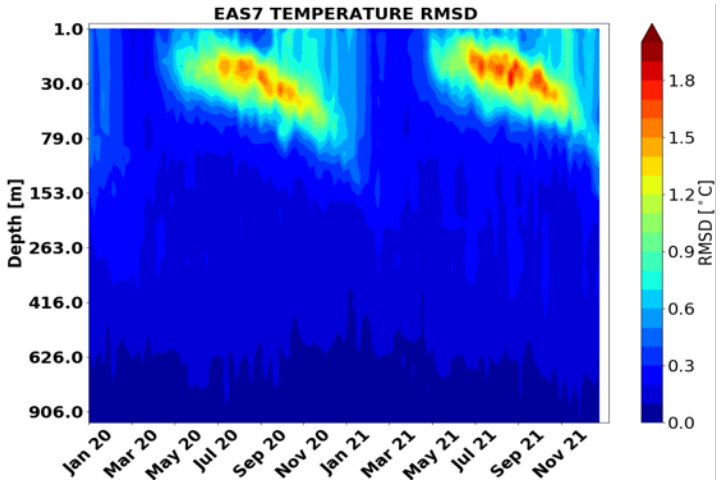

Figure 4: Hovmoller (Depth-Time) diagram of monthly mean RMS of temperature misfits along the water column averaged in the whole Mediterranean Sea during the two-years period 2020-2021 (T-<X-Y>m-2W-CLASS4–PROF-RMSD-MED- Jan2020-Dec2021-HOV).

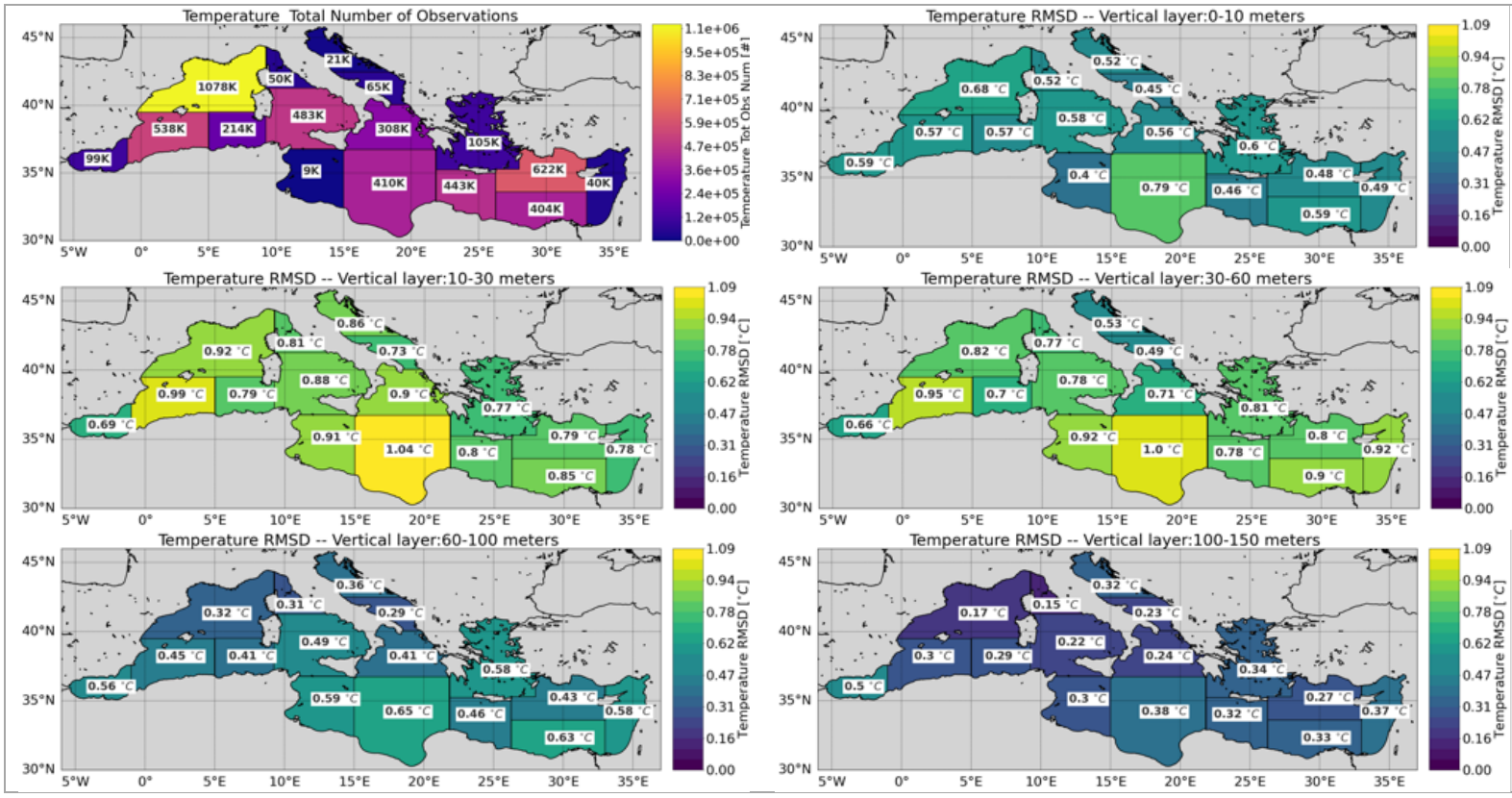

Figure 5: Maps of temperature RMSD per region computed on the entire qualification period (2020-2021). Top left: number of observations per region; top right and lower plots: RMSD respectively between 0-10 m, 10-30 m, 30-60 m, 60-100 m, 100-300 m, 300-600 m,600-1000 m and 1000-2000 m (T-<X-Y>m-2Y-CLASS4–PROF-RMSD-TS-Jan2020-Dec2021-2DMAP) (continues in next page).

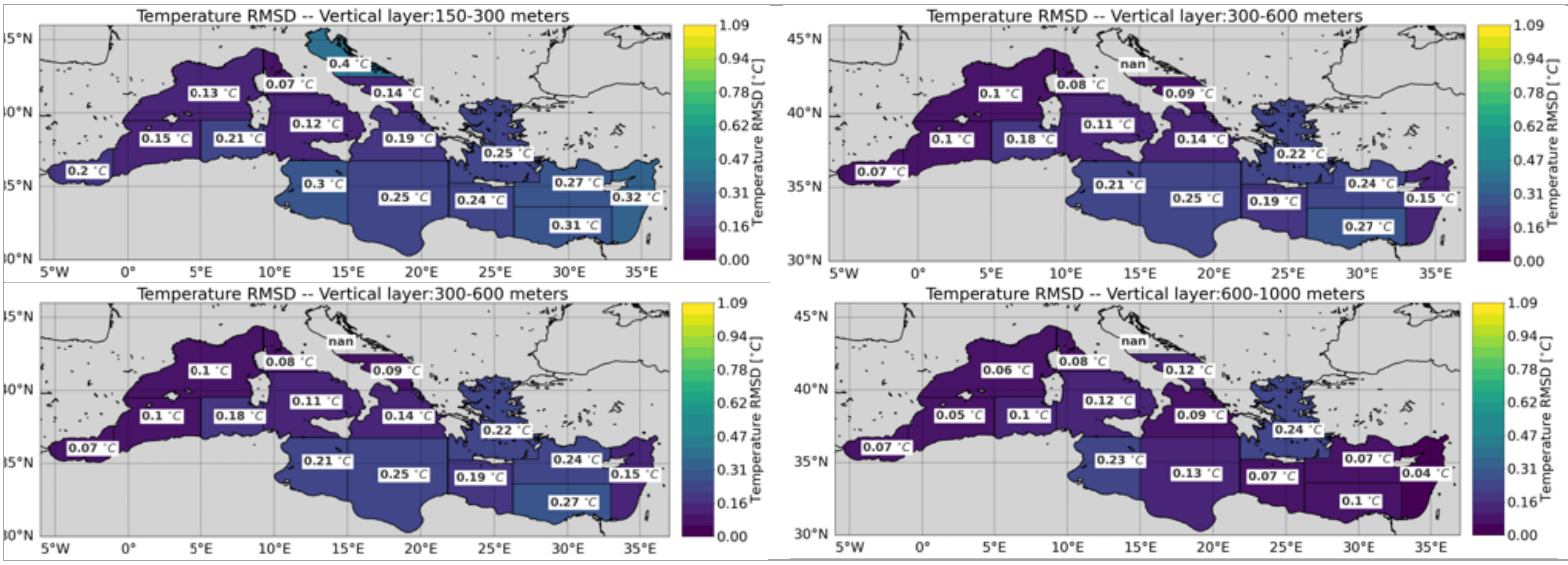

Figure 5: Maps of temperature RMSD per region computed on the entire qualification period (2020-2021). Top left: number of observations per region; top right and lower plots: RMSD respectively between 0-10 m, 10-30 m, 30-60m, 60-100 m, 100-300 m, 300-600 m,600-1000 m and 1000-2000m (T-<X-Y>m-2Y-CLASS4–PROF-RMSD-TS-Jan2020-Dec2021-2DMAP).

The following panels in Figure 6 show the time series of monthly temperature RMSD and Bias between observations and system outputs evaluated over the qualification period (2020-201) and depict the number of observations used for this validation (grey area). The statistics are evaluated for the 9 different layers (0-10, 10-30, 30-60, 60-100, 100-150, 150-300, 300-600, 600-1000, 1000-2000 m). The average value of RMSD over the entire period is also reported in the figure.

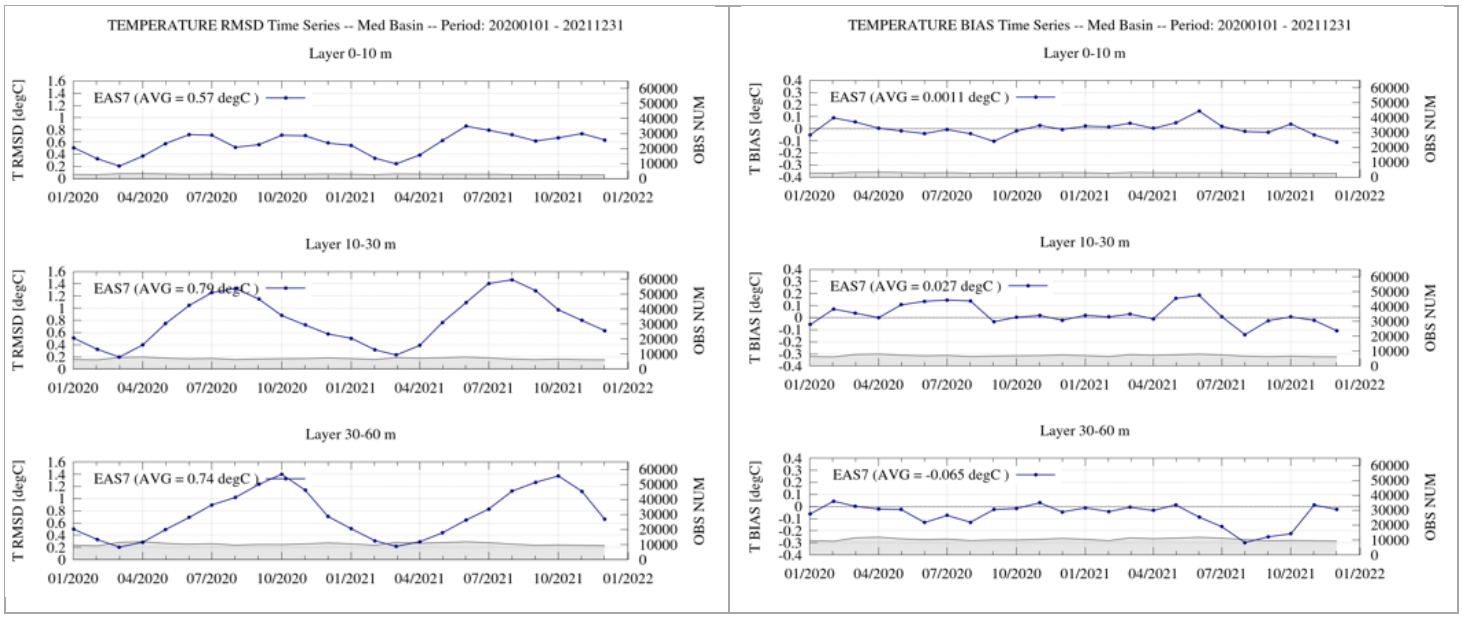

Figure 6: Time series of monthly RMSD (left panels) and bias (right panels) of temperature at different vertical layers (0-10, 10-30, 30-60, 60-100, 100-150, 150-300, 300-600, 600-1000, 1000-2000 m) for the two-years period 2020-2021 (continues in next page).

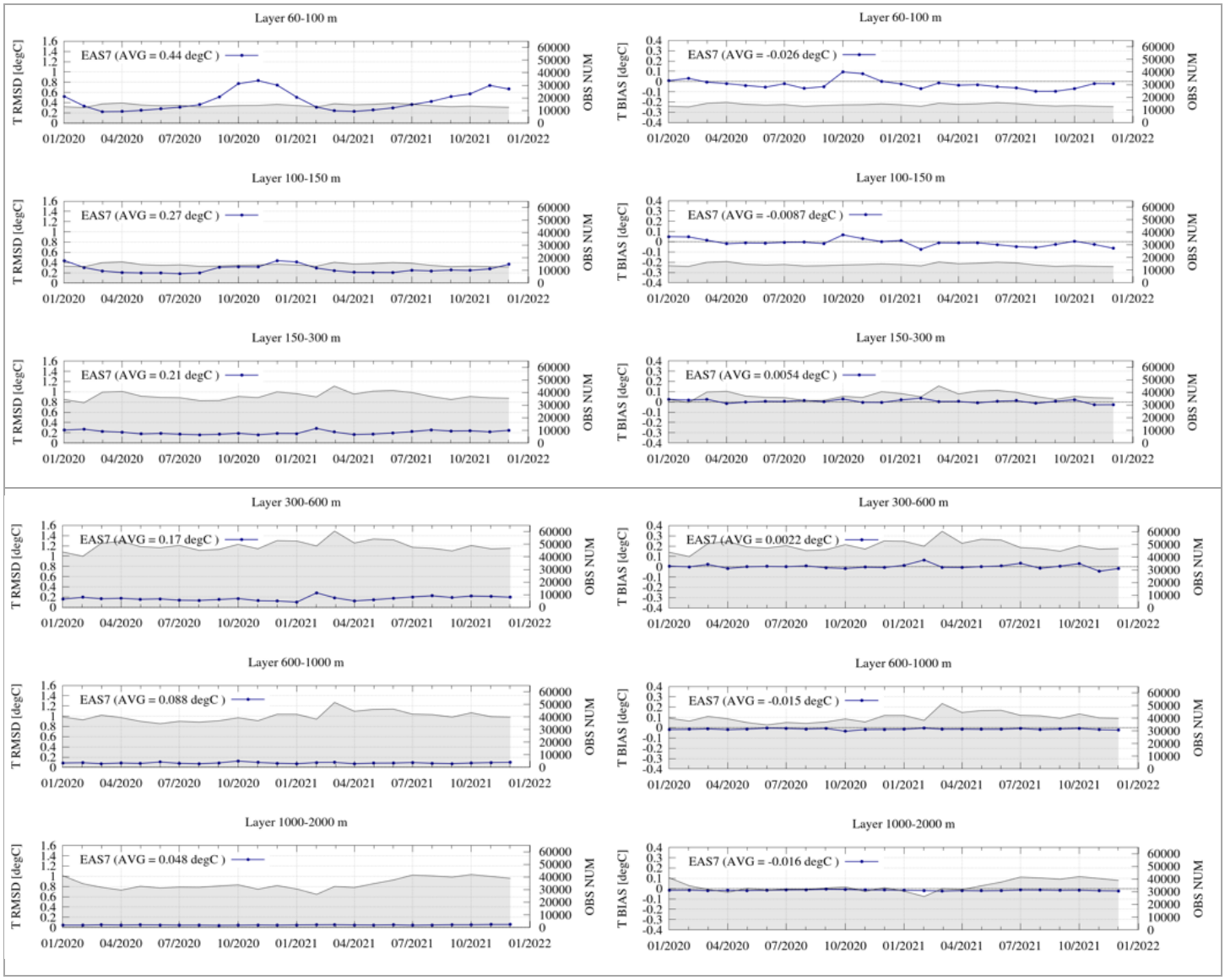

Figure 6: Time series of monthly RMSD (left panels) and bias (right panels) of temperature at different vertical layers (0-10, 10-30, 30-60, 60-100, 100-150, 150-300, 300-600, 600-1000, 1000-2000 m) for the two-years period 2020-2021.

The temperature error is generally higher above 100 m and presents a clear seasonal variability with higher values during warm seasons, then the error decreases significantly below 100 m and at lower levels.

Error! Reference source not found. Figure 7 shows the time series of daily RMS difference (solid line) and bias (dashed line) of Sea Surface Temperature of the system outputs with respect to observations (L4 satellite SST at 1/16° resolution) evaluated over the qualification testing period (Jan2020-Dec2021): SST-SURF-D-CLASS4-RAD-RMSD-Jan2020-Dec2021. The SST RMS difference is higher during the warm season while it presents a minimum during spring. The SST bias (observations – model) is generally negative meaning that the model presents a warmer SST with respect to the observations. It should be

noted that here daily mean EAS7 system outputs are compared to foundation SST (which is close to midnight SST).

Figure 8 depicts the SST EANs per region computed with respect to satellite data on the entire qualification period 2020-2021 along with the number of available observations per region. The largest errors are located in the south-Tyrrenian and Alboran Seas. The Alboran Sea shows a positive bias meaning that, in the area, the system is colder than the measured values.

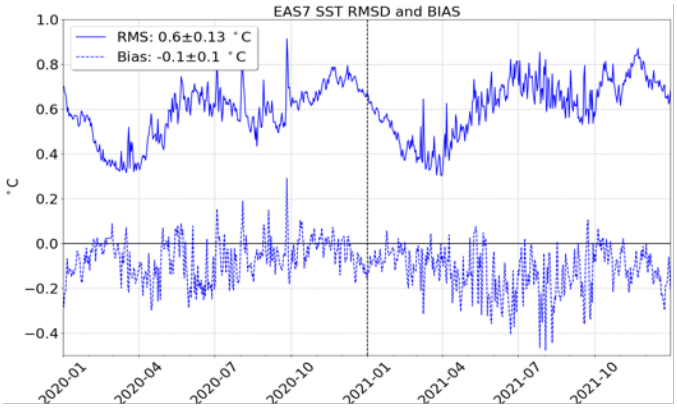

Figure 7: Time series of 2-weekly RMS difference (solid line) and Bias (dashed line) of Sea Surface Temperature (SST-D-CLASS4-RAD-RMSD-Jan2019-Dec2019, SST-D-CLASS4-RAD-BIAS-Jan2019-Dec2019) with respect to satellite L4 data at 1/16° resolution.

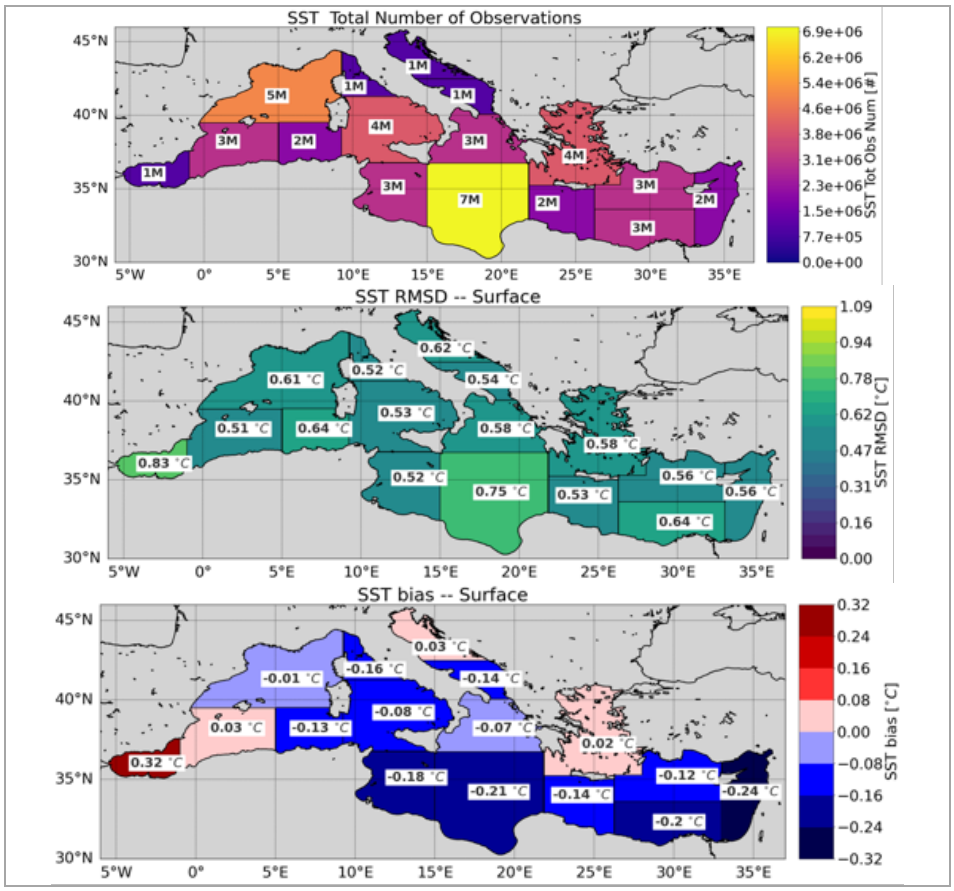

Figure 8: Map of SST RMSD (middle panel, SLA-SURF-W-CLASS4-ASSIM-ALT-RMSD-MED-Jan2020-Dec2021), bias (bottom panel), and number of observations (upper panel) per region computed with respect to satellite data on the entire qualification period 2020-2021 and map of the number of observations per region.

III.2 Seabed Temperature

The monthly climatology of bottom temperature, defined as the temperature of the deepest level of the circulation model, has been compared to SeaDataNet climatology (see Tonani et al., 2013 for more details) for the period 2020-2021.

Figure 9 shows the time series of the monthly climatological dataset (green lines) and EAS7 system (blue lines) evaluated as monthly averages for the two-years period. The left panel shows the climatological time series of seabed temperature obtained considering the depths between [0-500] m, while the right panel shows the comparison for depths between [0-1500] m. The system is able to reproduce the seasonal variability of the bottom temperature that is overestimated by the model with respect to the climatological dataset.

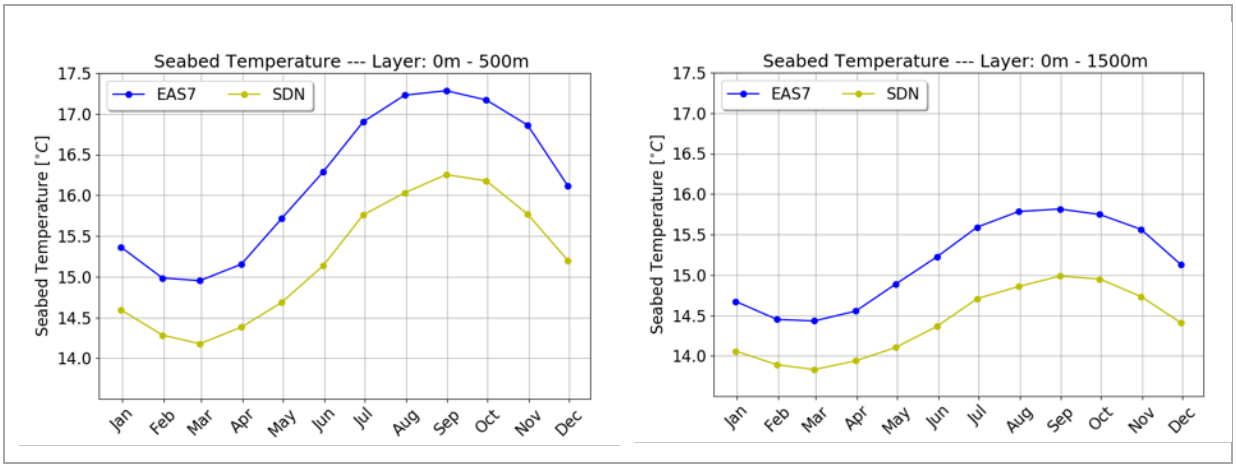

Figure 9: Time series of seabed temperature monthly climatology from SeaDataNet dataset (green line) and EAS7 system (blue line): SBT-D-CLASS4-CLIM-MEAN_M-MED.

The following figures show the January (Figure 10), April (Figure 11), July (Figure 12) and October (Figure **13**) monthly mean seabed temperature in areas where topography ranges between 0 and 1500 m from SDN dataset (left), and corresponding monthly averages for Med-Physics EAS7 system (right) evaluated for the two-years period 2020-2021. The system exhibits similar temporal and spatial patterns compared to the climatological datasets. The main differences are related to warmer seabed temperature along several coastal areas predicted by the EAS7 system with respect to the climatological dataset.

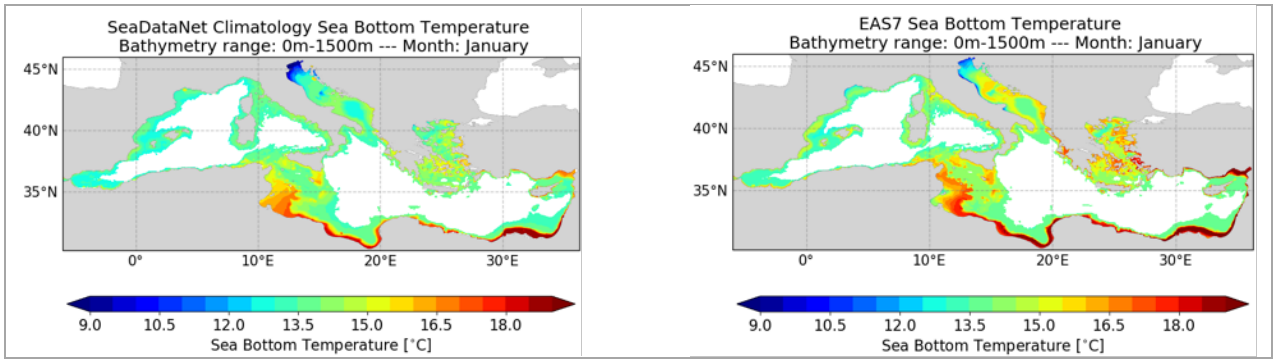

Figure 10: January Seabed temperature 2D maps in areas where topography is lower than 1500 m: SDN climatology (left), monthly average Med-Physics EAS7 system (right): SBT-D-CLASS1-CLIM-MEAN_M-MED.

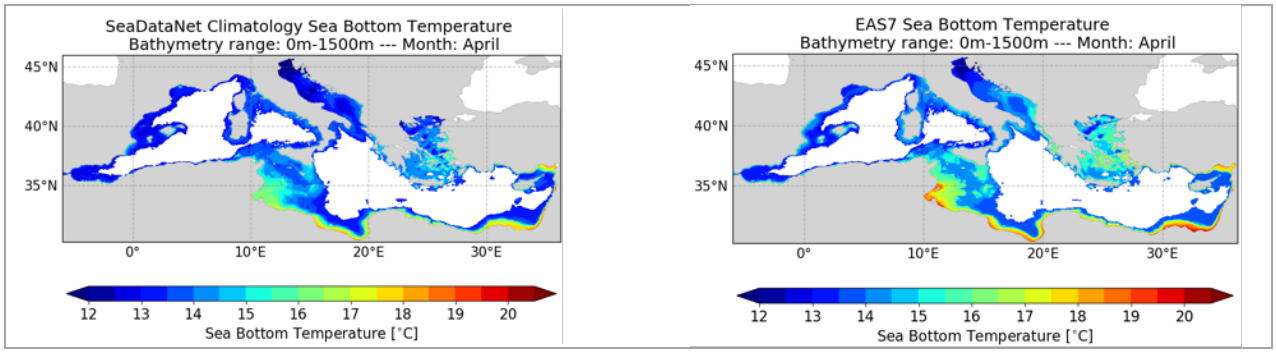

Figure 11: April Seabed temperature 2D maps in areas where topography is lower than 1500 m: SDN climatology (left), monthly average Med-Physics EAS7 system (right): SBT-D-CLASS1-CLIM-MEAN_M-MED.

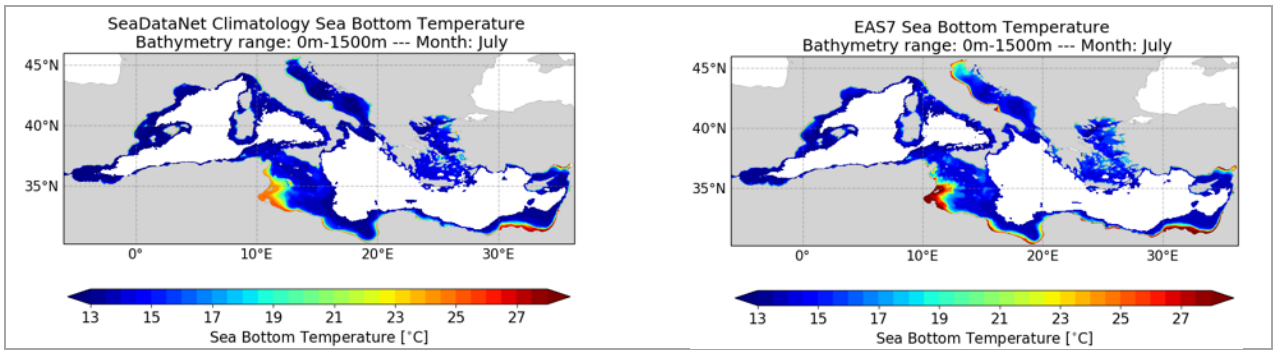

Figure 12: July Seabed temperature 2D maps in areas where topography is lower than 1500 m: SDN climatology (left), monthly average Med-Physics EAS7 system (right): SBT-D-CLASS1-CLIM-MEAN_M-MED.

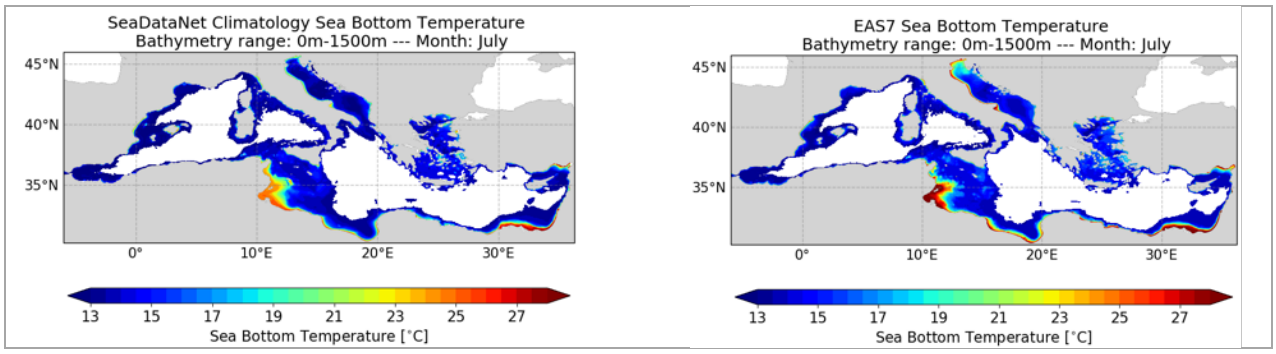

Figure 13: October Seabed temperature 2D maps in areas with topography lower than 1500 m: SDN climatology (left), monthly average Med-Physics EAS7 system (right): SBT-D-CLASS1-CLIM-MEAN_M-MED.

III.3 Salinity

In the following Table 8 there is a synthesis of the values of the salinity Root Mean Square (RMS) differences computed comparing the analysis of MEDSEA_ANALYSISFORECAST_PHY_006_013 product with quasi-independent data assimilated by the system for salinity (ARGO).

The synthesis is based on the two-years period 2020-2021 and it is provided at 5 depths (8, 30, 150, 300, 600 meters). The error is always lower than 0.17 PSU and it is higher at surface and decreases significantly below 150 m.

Variables/estimated accuracy:	Metrics	Depth	Observation
	RMS misfits [PSU]	**[m]**	**Instrument**
SALINITY	0.17 ± 0.03	8	Argo
	0.16 ± 0.03	30	Argo
	0.09 ± 0.02	150	Argo
	0.04 ± 0.01	300	Argo
	0.03 ± 0.00	600	Argo

Table 8: Quasi-independent validation. Analysis evaluation based over the two-years period 2020-2021.

The panels in Figure 14 show the time series of weekly RMS of salinity misfits (observation minus EAS7 system values transformed at the observation location and time before being assimilated) at 5 depths (8, 30, 150, 300, 600 m), S-<X-Y>m-2W-CLASS4- ASSIM–PROF-RMSD-MED-Jan2020-Dec2021; the values of the mean RMS differences are reported in the legend of the figures; the number of observed profiles that have been assimilated are represented as shaded areas.

The salinity error is generally higher above 30 m with mean values less than 0.17 PSU and better skill below 150 m with mean values lower than 0.1 PSU.

Monthly mean RMS of salinity misfits are represented in the following Figure 15 by means of Hovmoller diagrams (Depth-Time) along the water column between surface and 900 m depth showing the vertical pattern of the error averaged in the whole Mediterranean Sea. The system presents higher errors in the upper layers decreasing below 150 m.

In addition to basin averaged statistics, the following panels in Figure 16 show the spatial pattern of the salinity RMSD per subregion and per vertical layer, computed over the entire qualification period (2020-2021) with respect to ARGO data, S-<X-Y>m-2Y-CLASS4–PROF-RMSD-TS- Jan2020-Dec2021-2DMAP. The top right panel shows the number of observations along the whole water column used for this analysis. The maps confirm that the largest discrepancy appears between 10-100 m. The largest differences are located in the Aegean and South-Ionian Seas.

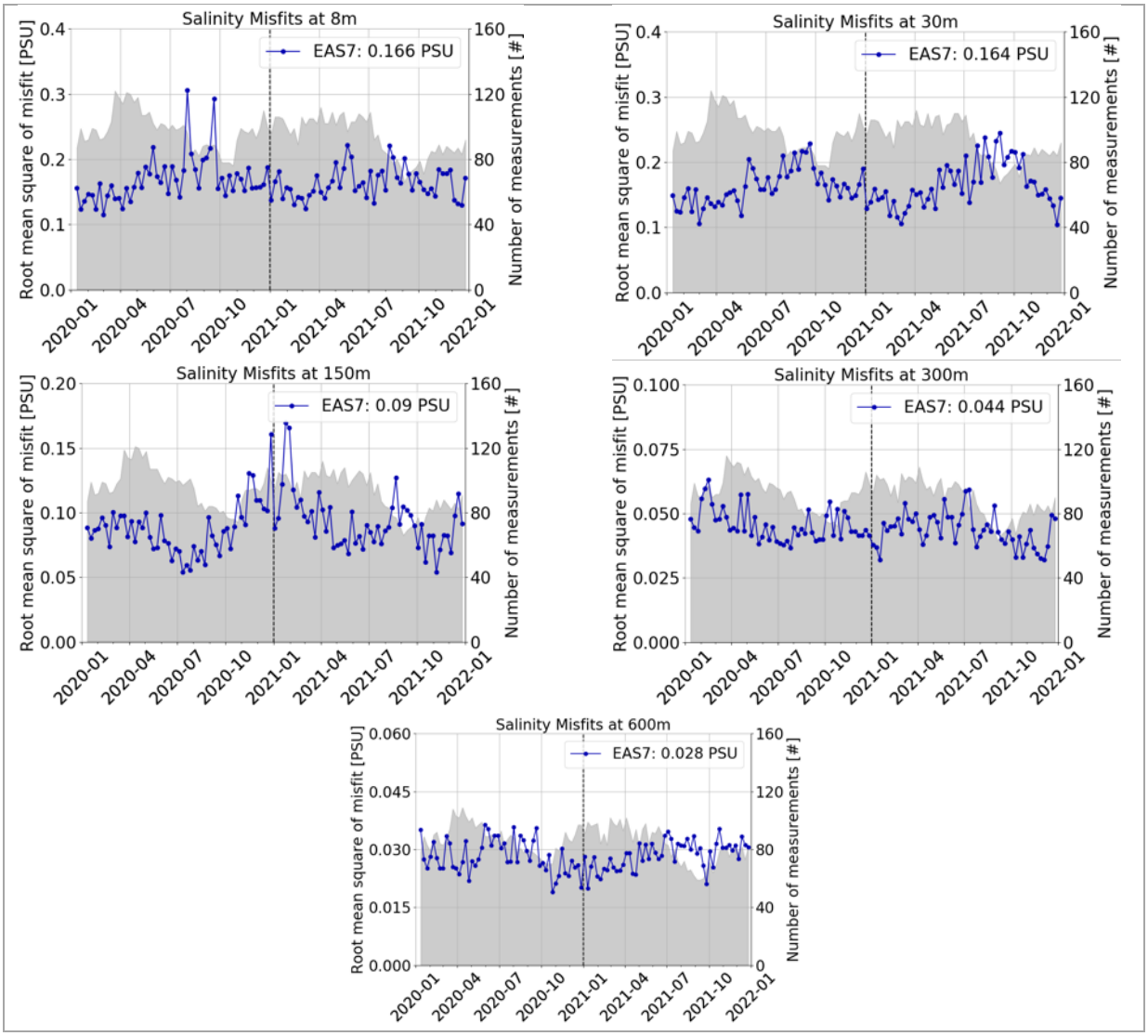

Figure 14: Time series of weekly RMS of salinity misfits (solid line) and number of observed profiles (shaded area) at 8, 30, 150, 300 and 600 meters (S-<X-Y>m-2W-CLASS4- ASSIM–PROF-RMSD-MED-Jan2020-Dec2021).

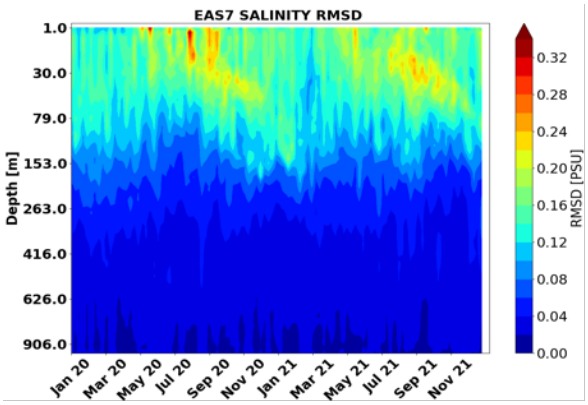

Figure 15: Hovmoller (Depth-Time) diagram of monthly mean RMS of salinity misfits along the water column averaged in the whole Mediterranean Sea during the two-years period 2020-2021 (S<X-Y>m-2W-CLASS4–PROF-RMSD-MED- Jan2020-Dec2021-HOV).

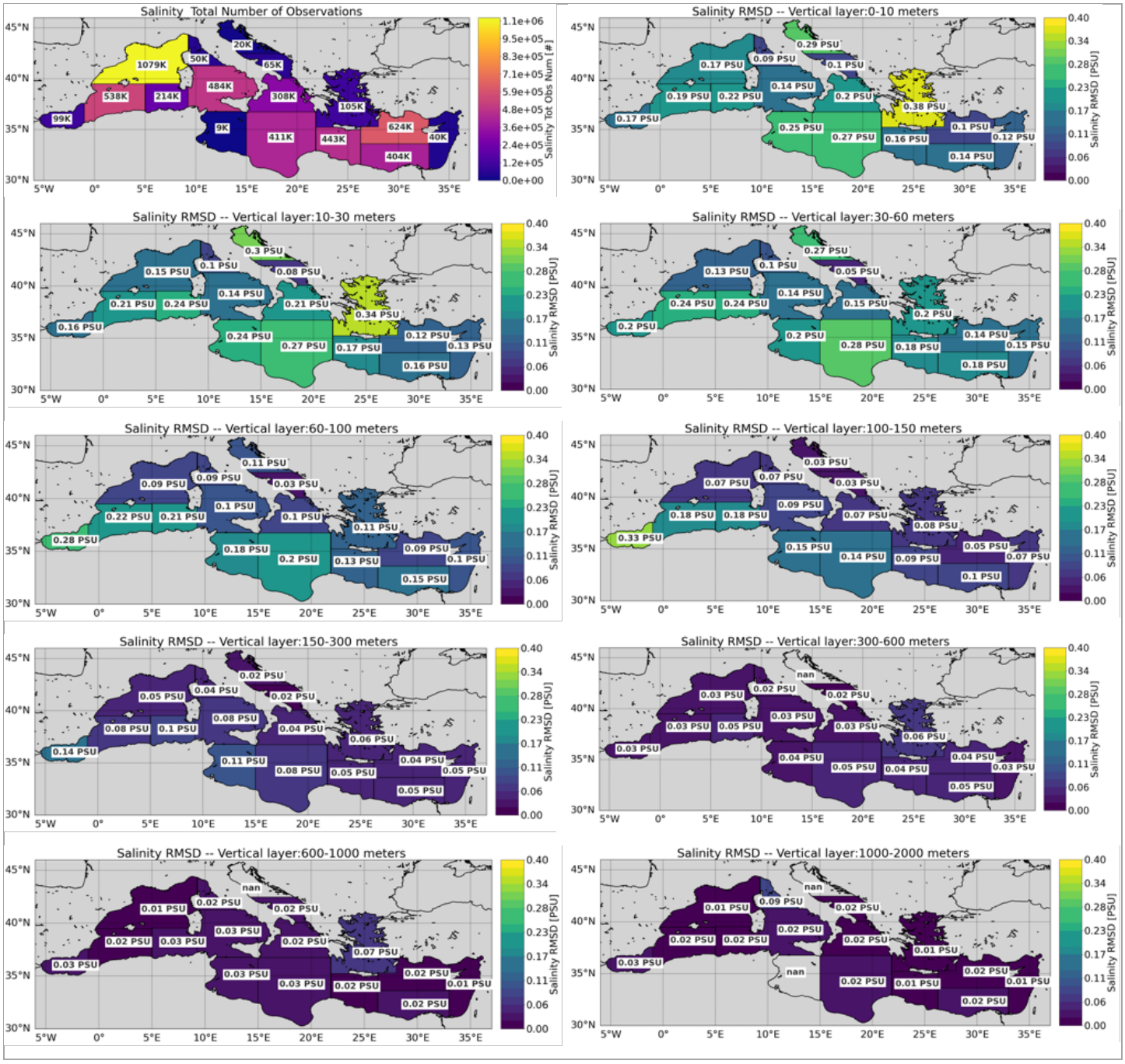

Figure 16: Maps of salinity RMSD per region computed on the entire qualification period (2020-2021). Top left: number of observations per region; top right and lower plots: RMSD respectively between 0-10 m, 10-30 m, 30-60 m, 60-100 m, 100-300 m, 300-600 m,600-1000 m and 1000-2000 m (S-<X-Y>m-2Y-CLASS4–PROF-RMSD-TS-Jan2020-Dec2021-2DMAP).

The following panels in Figure 17 show monthly salinity RMSD and Bias between observations and system outputs evaluated over the qualification period (2020-201) and depict the number of observations used for this validation (grey area). The statistics are evaluated for the 9 different layers (0-10, 10-30, 30-60, 60-100, 100-150, 150-300, 300-600, 600-1000, 1000-2000 m). Salinity error is generally higher above 150 m then the error decreases significantly below 150 m.

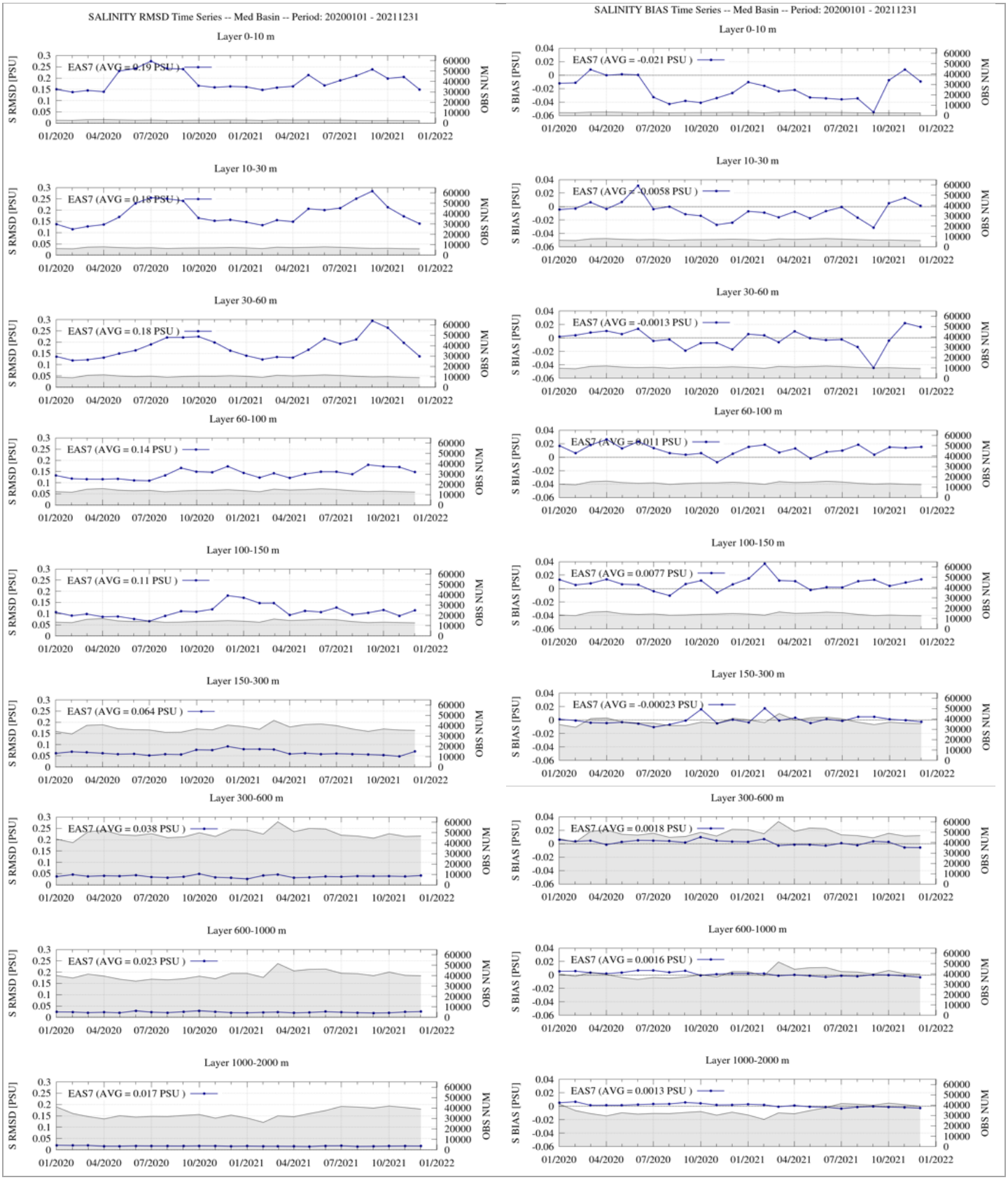

Figure 17: Time series of montly RMSD (left panels) and bias (right panels) of salinity at different vertical layers (0-10, 10-30, 30-60, 60-100, 100-150, 150-300, 300-600, 600-1000, 1000-2000 m) for the two-years period 2020-2021.

III.4 Sea Level

In Table 9 the RMS differences for the Sea Level Anomaly computed comparing the analysis of MEDSEA_ANALYSISFORECAST_PHY_006_013 product with each available satellite (along track observations) from January 2020 to December 2021 are given.

Satellite	SLA RMS Diff [cm]	Availability	Num of missing days
All Satellites	3.0±0.2	01/01/2020-31/12/2021	0
ALTIKA	2.9±0.3	01/01/2020-31/12/2021	0
CRYOSAT 2	3.0±0.3	01/01/2020-31/12/2021	1 day gap
JASON 3	3.0±0.3	01/01/2020-31/12/2021	1 day gap
SENTINEL 3A	3.0±0.3	01/01/2020-31/12/2021	0
SENTINEL 3B	3.0±0.3	01/01/2020-31/12/2021	0
HY-2A	3.1±0.3	01/01/2020-14/06/2020	80 days gap
HY-2B	3.0±0.4	01/01/2020-31/12/2021	5 days gap

Table 9: Analysis evaluation based on the two-years time series 2020-2021 for Sea Level Anomaly for each available satellite.

Figure 18 depicts the SLA RMSD per subregion, computed with respect to satellite data on the entire qualification period 2020-2021 along with the number of available observations per region. High differences correspond to regions characterized by a low availability of data, e.g. the Alboran Sea.

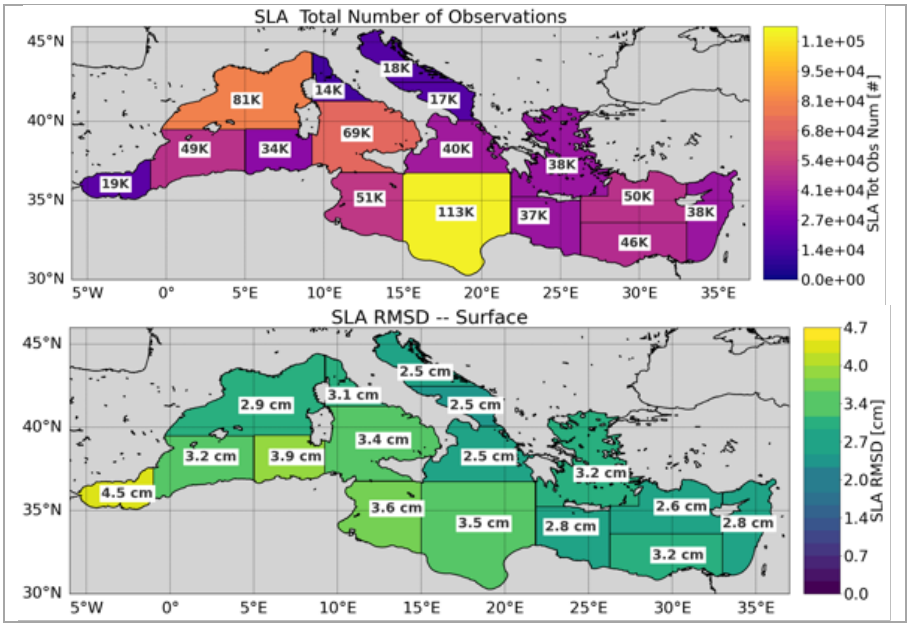

Figure 18: Map of SLA RMSD (lower panel) and number of observations (upper panel) per region computed with respect to satellite data on the entire qualification period 2020-2021 and map of the number of observations per region.

The following Figure 19 shows the time series of bi-weekly RMS differences of sea level anomaly misfits (observation minus model value transformed at the observation location and time before being assimilated), SLA-SURF-2W-CLASS4-ASSIM-ALT-RMSD-MED-Jan2020-Dec2021. The number of assimilated data is provided as shaded area. The system has an overall error of about 3.0 cm in the whole basin.

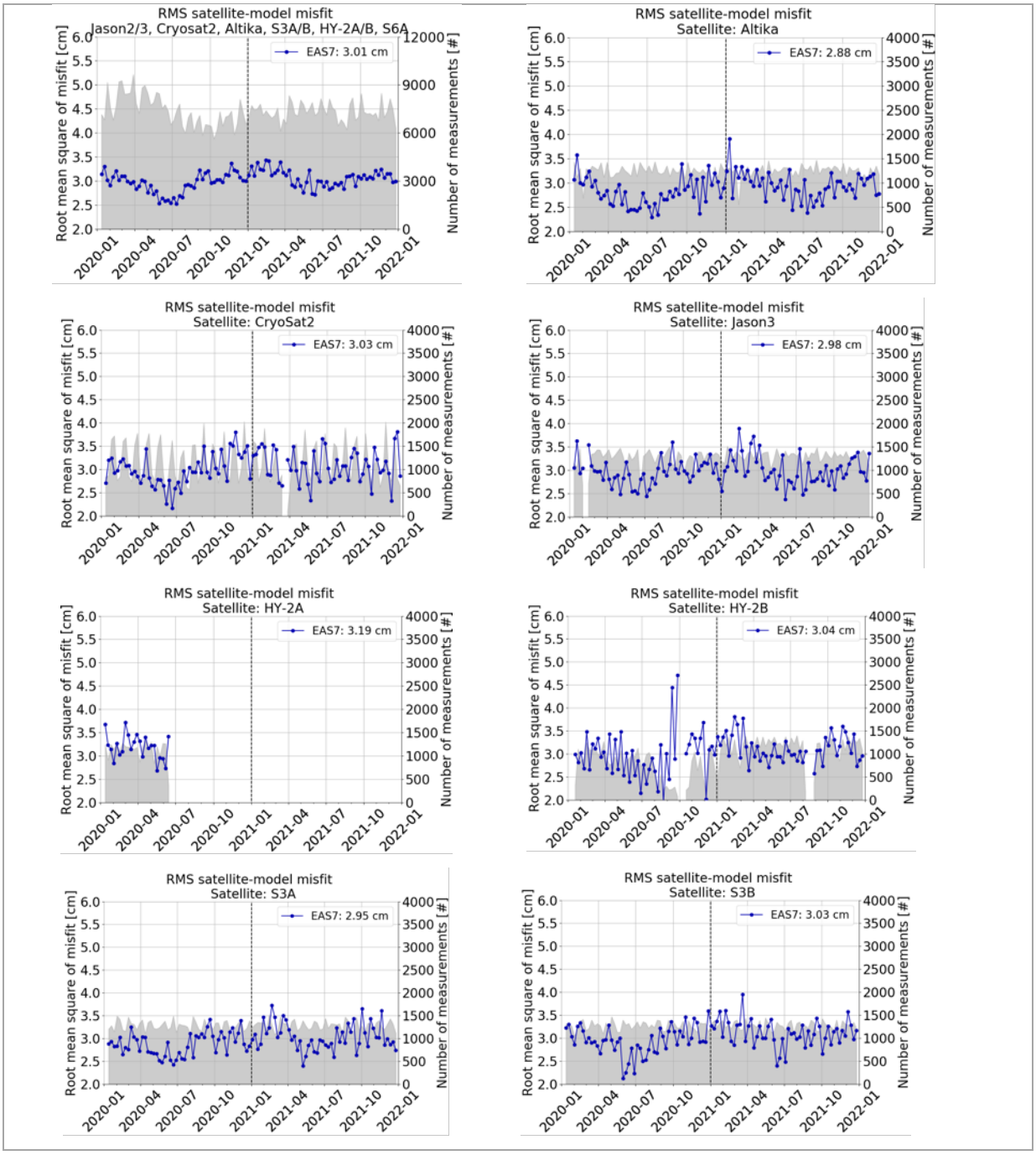

Figure 19: Time series of weekly RMS of misfits along SLA data track for all the satellites, Altika, Cryosat, Jason2G, Jason3, Sentinel3A, Sentinel3B, HY-2A, HY-2B, Sentinel6A and the corresponding number of assimilated data (shaded areas in the Figures) (SLA-SURF-2W-CLASS4- ASSIM-ALT-RMSD-MED-Jan2020-Dec2021).

III.5 Currents

The predicted sea surface currents skill is assessed by means of independent validation through coastal moorings.

Table 10 summarizes the RMS differences and the bias obtained comparing the analysis of MEDSEA_ANALYSISFORECAST_PHY_006_013 product with the available independent in-situ data: five coastal moored buoys for the period 2020-2021. Moreover in Figure 20 the scatter plot, model output VS observed values, is shown together with the resulting statistics. The location of the moorings is showed in Figure 21. All the time-series concern a depth ranging between 0 and 3 meters. Due to the reduced number of observations, mainly located in coastal areas of the west side of the basin, the statistical relevance of currents performance is poor.

Variable	RMS diff	Bias	Depth	No. of available buoys
	UV-SURF-D-CLASS2-MOOR-RMSD-Jan2020-Dec2021	UV-SURF-D-CLASS2-MOOR-BIAS-Jan2020-Dec2021		
EAS7 Current	0.13 m/s	-0.07 m/s	0-3 m	6

Table 10: Independent observation evaluation based on the two-years time series 2020-2021 of analysis and Moored Buoys observations.

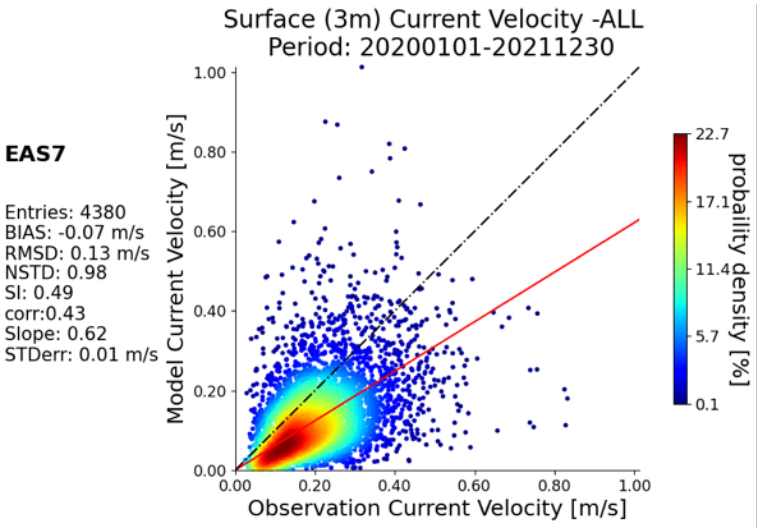

Figure 20: Scatter plot between EAS7 currents and observed velocity values in 2020-2021 and statistical values resulting from the comparison.

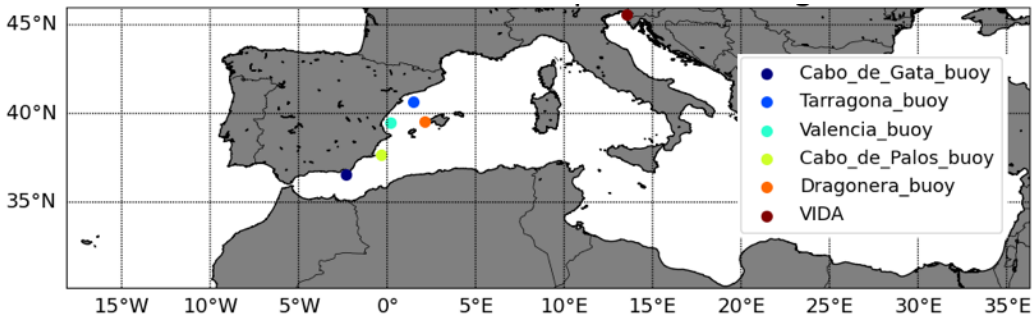

Figure 21: Location of the five moorings available for validation in 2020-2021

Figure 22 shows an example of daily sea surface currents time series of EAS7 (blue line) daily mean model outputs against the Cabo de Gata coastal mooring (orange line) for period 2020-2021, the figure includes also the mean values.

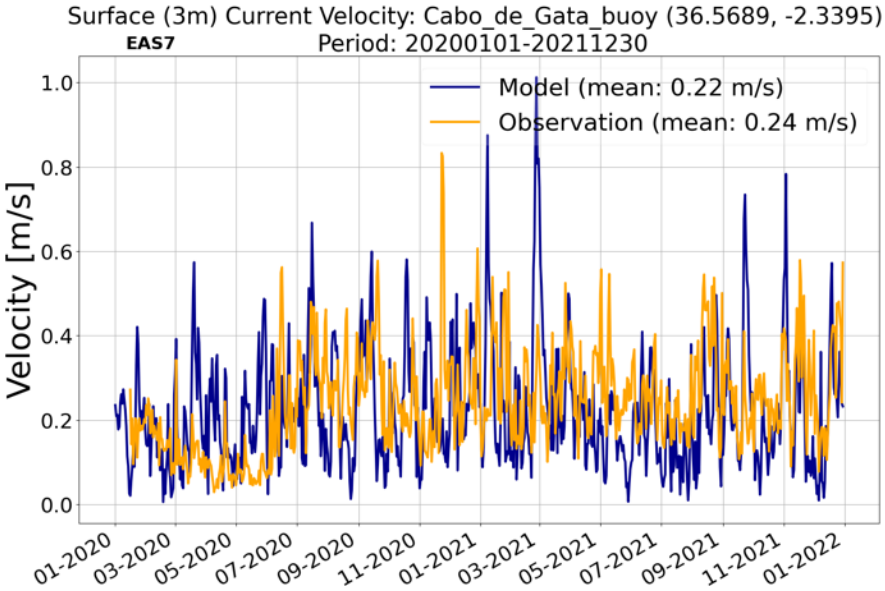

Figure 22: Time series of surface currents at Cabo de Gata buoy. Comparison between observations (orange line) and EAS7 model outputs (blue line). (UV-SURF-D-CLASS2-MOOR-RMSD-Jan2020-Dec2021, UV-SURF-D-CLASS2-MOOR-BIAS-Jan2020-Dec2021).

In addition to surface current validation, an assessment of velocity derived variables is provided in terms of transport through the strait of Gibraltar.

In Figure 23 the time series of the mean daily net, eastward and westward fluxes through the Gibraltar Strait in the 7-years period 2016-2021 are represented. The values of the transports are computed by means of an on-line procedure.

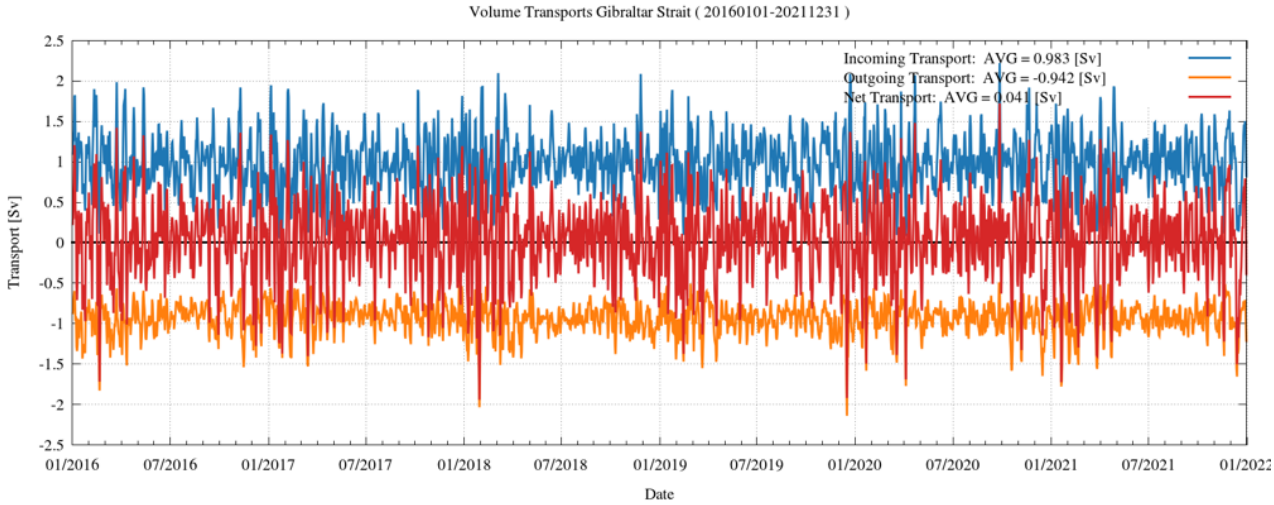

Figure 23: Time series of daily mean Net (red), Eastward (blue) and Westward (orange) fluxes through the Gibraltar Strait in 2016-2021.

In

Table **11** the comparison of the mean net, eastward and westward transports across the 5°48' W section with respect to literature fluxes (Soto-Navarro et al., 2010) is included. The literature values have been estimated measuring the currents form October 2004 to January 2009 across the 5°58.60' W section. In order to compare these values with literature, in addition to the 2020-2021 mean transports, a longer period evaluation has been reported showing the seven year mean (2016-2021) transports.

Gibraltar Mean Transport	EAS7 (2020-2021)	EAS7 (2016-2021)	Soto-Navarro et al., 2010
Net	0.042 Sv	0.041 ± 0.010 Sv	0.038 ± 0.007 Sv
Eastward	0.99 Sv	0.98 ± 0.02 Sv	0.81 ± 0.06 Sv
Westward	0.94 Sv	0.94 ± 0.03 Sv	0.78 ± 0.05 Sv

Table 11: Gibraltar strait mean fluxes for EAS7 system averaged on 2020-2021 and on a longer period (2016-2021) compared to literature values (Soto-Navarro et al. 2010).

III.6 Mixed Layer Depth

In order to assess the EAS7 system ability to reproduce the Mixed Layer Depth (MLD), 2D maps of MLD monthly average computed on the five-years period 2017-2021, have been compared to a climatological dataset available from literature (Houpert et al., 2015) providing monthly gridded climatology produced using MBT, XBT, Profiling floats, Gliders, and ship-based CTD data from different database and carried out in the Mediterranean Sea between 1969 and 2013. Figure 24 to Figure 27 show the 2D maps of climatological MLD from literature (top), monthly averaged (over the five-years period 2017-2021) MLD from MED-Physics EAS7 system (bottom).

It can be noticed that in February (Figure 24), the deepening of the MLD in the Gulf of Lyon and in the South Adriatic areas are represented by EAS7 system, which present a deeper MLD in the Aegean See than the one shown in the climatological fields. During June and August (Figure 25: and Figure 26:) the modelled MLD is in general similar to the climatological one showing a slightly higher mean value of the MLD especially in June. In December (Figure 27:) the deepening of the MLD is well represented by the EAS7 system, the Gulf of Lyon, Adriatic and Aegean deepening of the MLD are more enhanced with respect to the MLD climatology.

In general, it can be noticed that the EAS7 numerical system is able to represent the spatial and seasonal distribution of the MLD and the main differences can be due to the low resolution of the climatological dataset that moreover do not cover the whole domain of the Mediterranean Sea as well as on the different period of evaluation, being the Mediterranean Sea characterized by areas of deep-water formation whose deepening can significantly vary in time. In particular, the different extensions of the area characterized by the deepening of the MLD may be due to the duration of the period on which the average is computed.

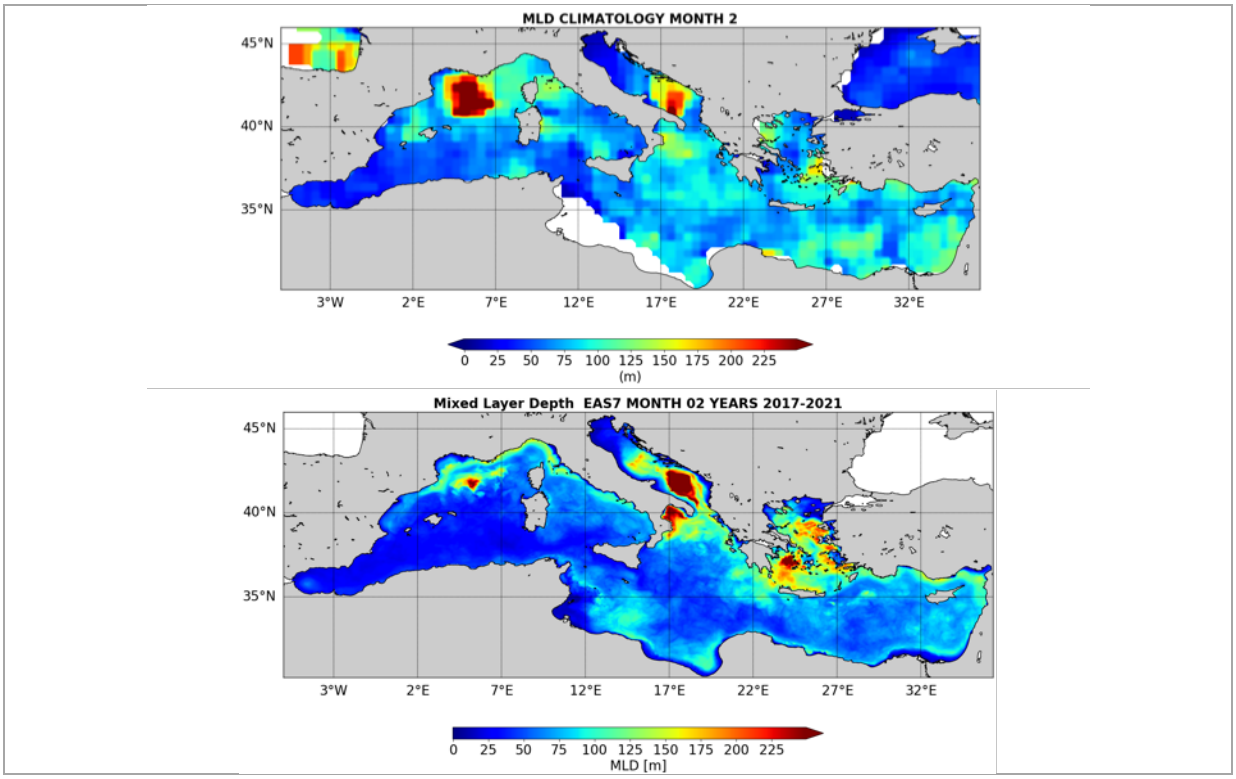

Figure 24: February MLD 2D maps. Top: climatological data from literature; bottom: February 2017-2021 monthly averaged MLD from MED-Physics EAS7 system: MLD-D-CLASS1-CLIM-MEAN_M-MED.

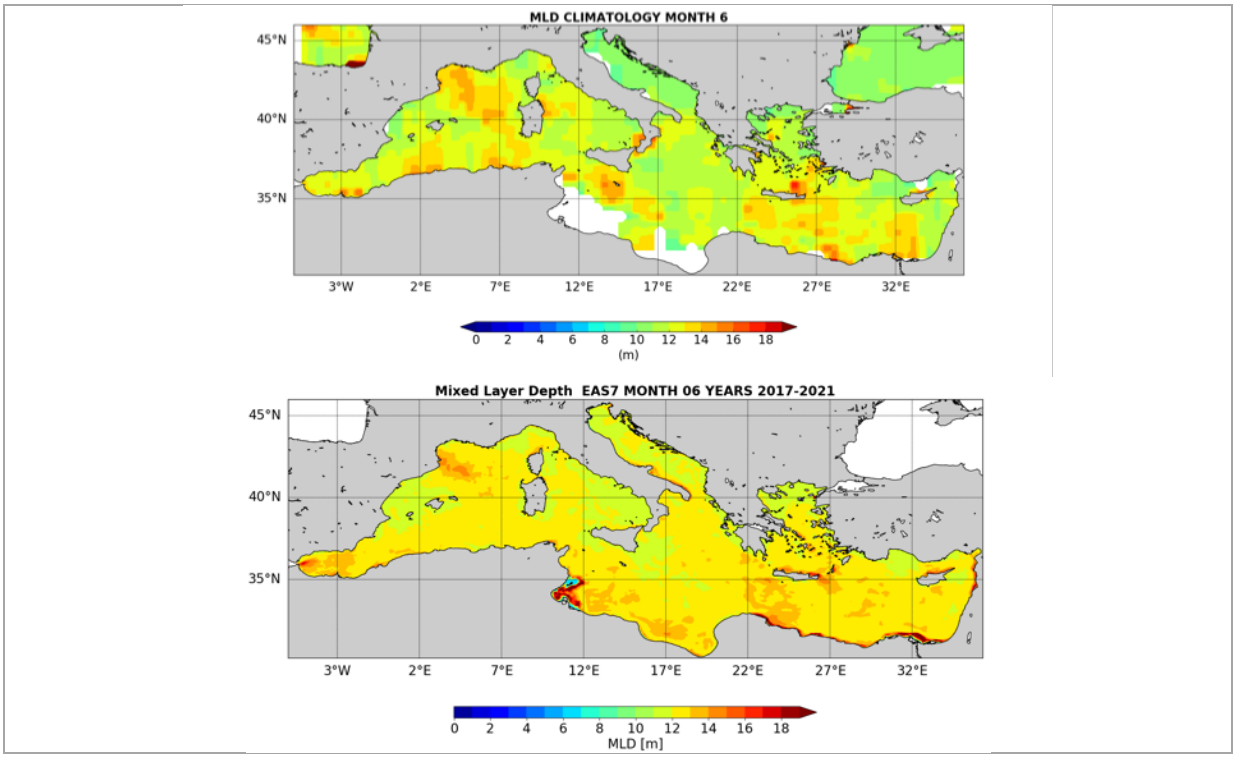

Figure 25: June MLD 2D maps. Top: climatological data from literature; bottom: June 2017-2021 monthly averaged MLD from MED-Physics EAS7 system: MLD-D-CLASS1-CLIM-MEAN_M-MED.

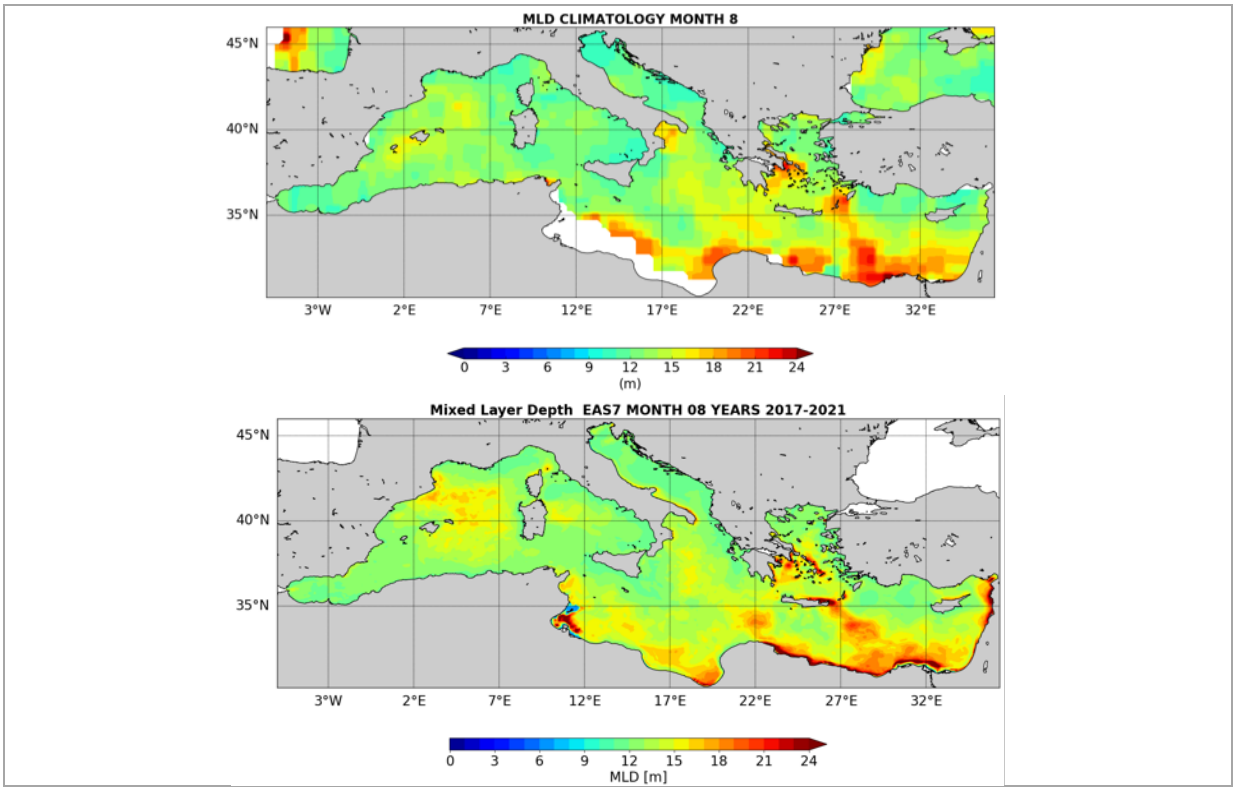

Figure 26: August MLD 2D maps. Top: climatological data from literature; bottom: August 2017-2021 monthly averaged MLD from MED-Physics EAS7 system: MLD-D-CLASS1-CLIM-MEAN_M-MED.

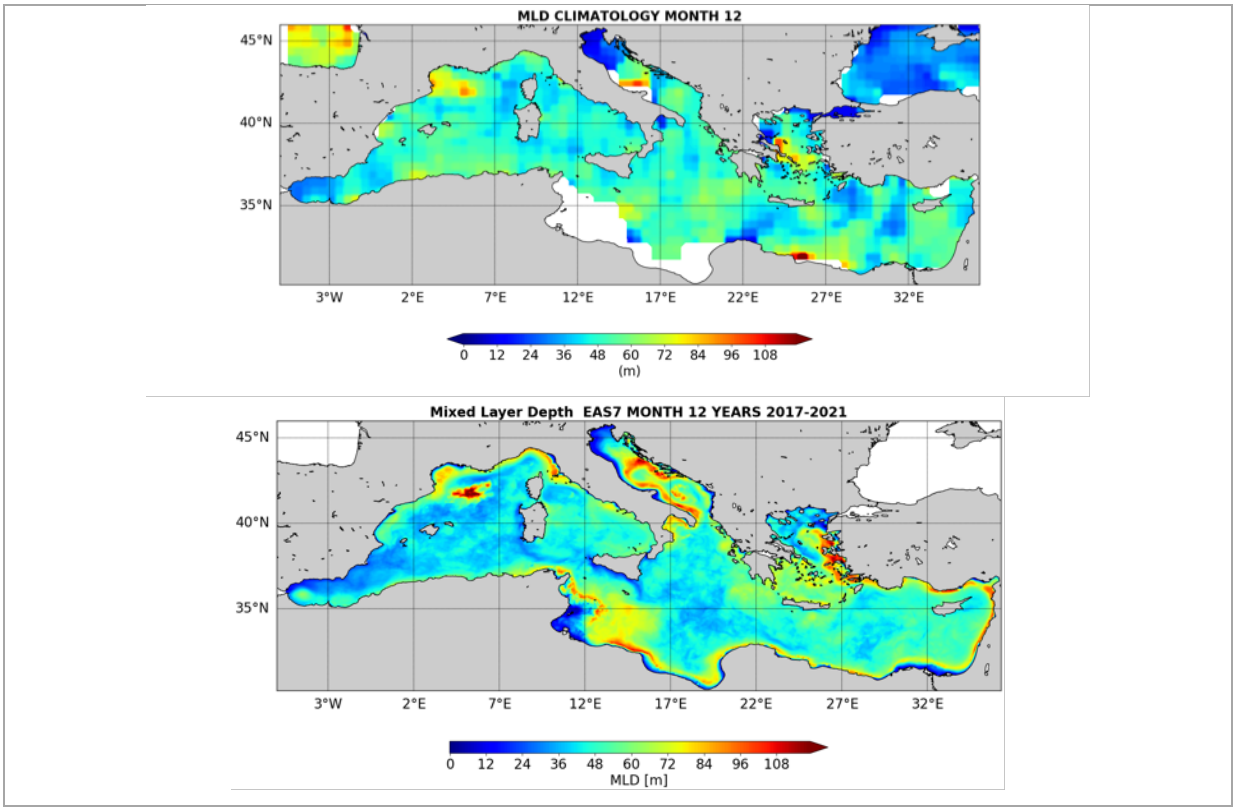

Figure 27: December MLD 2D maps. Top: climatological data from literature; bottom: December 2017-2021 monthly averaged MLD from MED-Physics EAS7 system: MLD-D-CLASS1-CLIM-MEAN_M-MED.

III.7 Harmonic Analysis

A specific analysis has been performed to evaluate the quality of EAS7 system which includes tides to verify its ability to reproduce the tidal amplitudes and phases of each tidal component. This validation analysis is performed by means of an harmonic analysis based on six-months period of hourly sea level field. Figure 28 shows the location of the tide gauges that have been used for this analysis, different colours represent different areas of the basin, while the numbers refer to the tide gauges listed in the following Table 12.

Figure 29 shows the amplitude and phase scatter plots for the 4 major tidal constituents: M2, S2, K1, O1 EAS7 system versus Observations. This analysis shows very good agreement between the model and observations.

The error bars in the scatter plots represent the errors on amplitudes and phases of modelled and observed values. The errors arise in the harmonic analysis procedure used to compute amplitudes and phases from a sea-surface-hight time-series. In particular we use the Foreman methodology which is basically a fit procedure. The errors given in the plots are boostrapped 95% confidence intervals based on an uncorrelated bivariate coloured-noise model.

The errors on the harmonic analysis output, namely on amplitude and phase values, can reach a magnitude of several centimetres/degrees. Since the order of magnitude of the amplitude of diurnal components such as K1 and O1 is respectively lower than 20 and 10 centimetres, the error becomes non negligible with respect to the values.

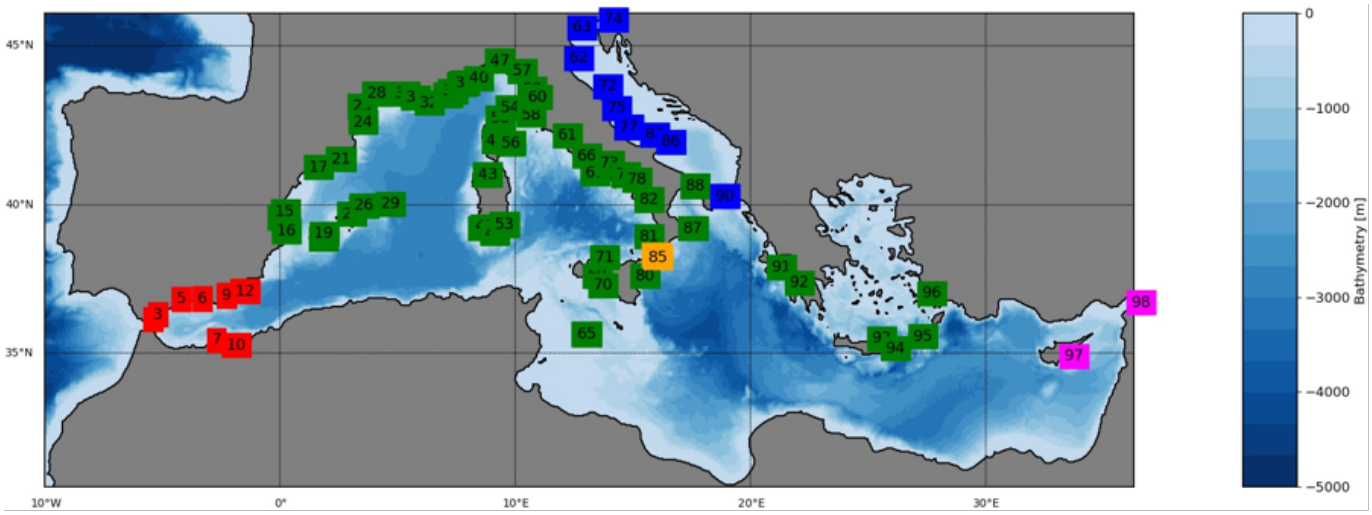

Figure 28: Location of the Mediterranean tide gauges used to perform the harmonic analysis.

Name	Label	Longitude	Latitude
TarifaTG	1	-5.6036	36.0064
IOC_alge	2	-5.3984	36.177
AlgecirasTG	3	-5.3983	36.1769
IOC_mal3	4	-4.4171	36.7118
MalagaTG	5	-4.417	36.712
IOC_motr	6	-3.5236	36.7202
MelillaTG	7	-2.918	35.291
Almeria2TG	8	-2.4809	36.8319
IOC_alme	9	-2.4784	36.83
IOC_said	10	-2.2929	35.1119
CarbonerasTG	11	-1.8996	36.9743
IOC_carb	12	-1.8996	36.9743
ValenciaTG	13	-0.33	39.46
IOC_vale	14	-0.3113	39.442
SaguntoTG	15	-0.206	39.634
GandiaTG	16	-0.152	38.995
TarragonaTG	17	1.2132	41.0789
FormenteraTG	18	1.4189	38.7347
IbizaTG	19	1.4497	38.9111
BarcelonaTG	20	2.163	41.342
IOC_barc	21	2.1657	41.3418
PalmadeMallorcaTG	22	2.6375	39.5603
PortLaNouvelleTG	23	3.0641	43.0147
IOC_ptve	24	3.1073	42.5201
IOC_alcu	25	3.139	39.8346
AlcudiaTG	26	3.1392	39.8347
IOC_sete	27	3.6991	43.3976
SeteTG	28	3.7017	43.4
MahonTG	29	4.2706	39.893
FosSurMerTG	30	4.8929	43.4049
MarseilleTG	31	5.3537	43.2785
IOC_toul2	32	5.9131	43.1172
PortFerreolTG	33	6.7176	43.3591
IOC_figu	34	6.9338	43.4835
IOC_figu2	35	6.9338	43.4835
LaFigueirettеTG	36	6.9338	43.4835
IOC_nice2	37	7.285	43.695
NiceTG	38	7.2855	43.6956
MonacoTG	39	7.4237	43.733
IOC_IM01	40	8.0188	43.8769
TAD_ISPRA-17	41	8.1829	39.0837
IOC_CF06	42	8.3081	39.1436
RMN-PortoTorres	43	8.4039	40.8422
TAD_IDSL-09	44	8.7195	38.9275
AjaccioTG	45	8.7629	41.9227
IOC_GE25	46	8.9255	44.4101
RMN-Genova	47	8.9255	44.4101
IleRousseTG	48	8.9352	42.6396
IOC_rous2	49	8.9381	42.6356
IOC_rous	50	8.9381	42.6356
IOC_CA02	51	9.1142	39.2101
RMN-Cagliari	52	9.1142	39.2101
TAD_ISPRA-07	53	9.1143	39.2102
CenturiTG	54	9.3498	42.9658
IOC_sole2	55	9.3738	41.8358
SolenzaraTG	56	9.4038	41.8569
IOC_LA38	57	9.8576	44.0966
RMN-MarinaDiCampo	58	10.2383	42.7426
RMN-Livorno	59	10.2993	43.5463
TAD_ISPRA-14	60	10.5333	43.2913
RMN-Civitavecchia	61	11.7896	42.094
RMN-Ravenna	62	12.2829	44.4921
RMN-Venice	63	12.4265	45.4182
TAD_ISPRA-11	64	12.604	35.5
IOC_LA23	65	12.6044	35.4998
RMN-Anzio	66	12.6348	41.4469
RMN-Ponza	67	12.9656	40.8952
RMN-Sciacca	68	13.0765	37.5045
TAD_ISPRA-12	69	13.0765	37.5045
TAD_ISPRA-16	70	13.3128	37.1725
RMN-Palermo	71	13.3713	38.1214
RMN-Ancona	72	13.5065	43.6248
RMN-Gaeta	73	13.5897	41.21
RMN-Trieste	74	13.7561	45.6544
RMN-SBenedettoDelTronto	75	13.8898	42.9551
RMN-Napoli	76	14.2692	40.8397
RMN-Ortona	77	14.4149	42.3559
TAD_ISPRA-03	78	14.7508	40.6766
IOC_CT03	79	15.0938	37.498
RMN-Catania	80	15.0938	37.498
TAD_ISPRA-01	81	15.2517	38.8173
RMN-Palinuro	82	15.2753	40.0299
RMN-IsoleTremiti	83	15.5016	42.1189
TAD_ISPRA-10	84	15.5635	38.1963
TAD_ISPRA-09	85	15.6489	38.1217
RMN-Vieste	86	16.177	41.8881
TAD_ISPRA-08	87	17.137	39.0816
RMN-Taranto	88	17.2238	40.4756
RMN-Otranto	89	18.4969	40.1464
TAD_ISPRA-15	90	18.497	40.146
TAD_NOA-07	91	20.9052	37.7814
TAD_NOA-08	92	21.6644	37.2596
TAD_NOA-10	93	25.1525	35.3484
TAD_NOA-04	94	25.7385	35.0037
TAD_NOA-03	95	26.9218	35.4186
TAD_IDSL-25	96	27.2878	36.8984
IOC_zygi1	97	33.3402	34.7263
IOC_iske	98	36.1768	36.5942

Table 12: List of the 98 EMODnet tide gauges used to perform the harmonic analysis: name, number and coordinates. The colours correspond to different areas of the basin (see Figure 28:) and, the ones in bold, correspond to the dataset whose values are available also in literature.

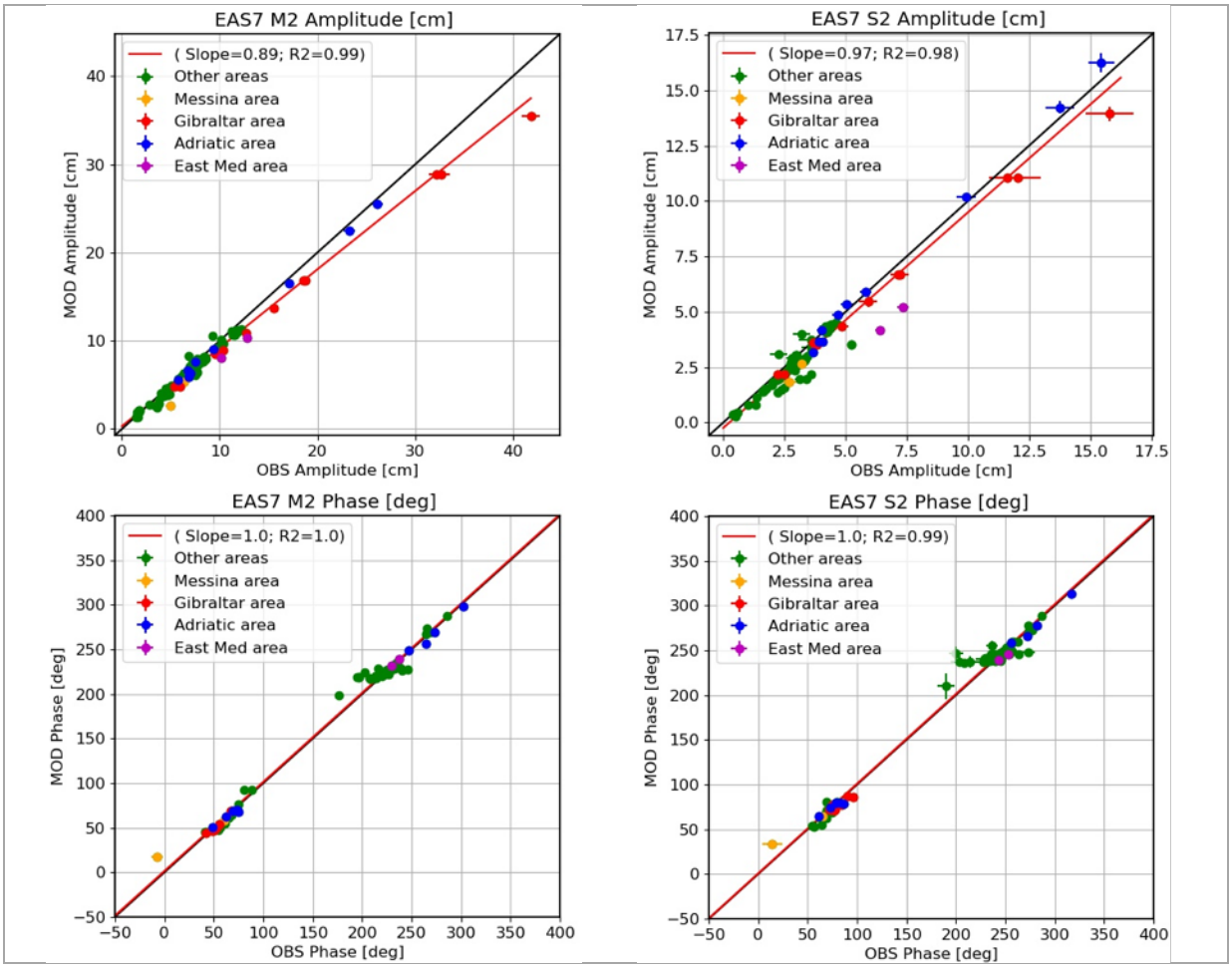

Figure 29: Scatter plot of tidal amplitude and phase for the 4 major Mediterranean Sea tidal constituents: M2, S2, K1, O1 evaluated at 98 tide gauges (continues in next page).

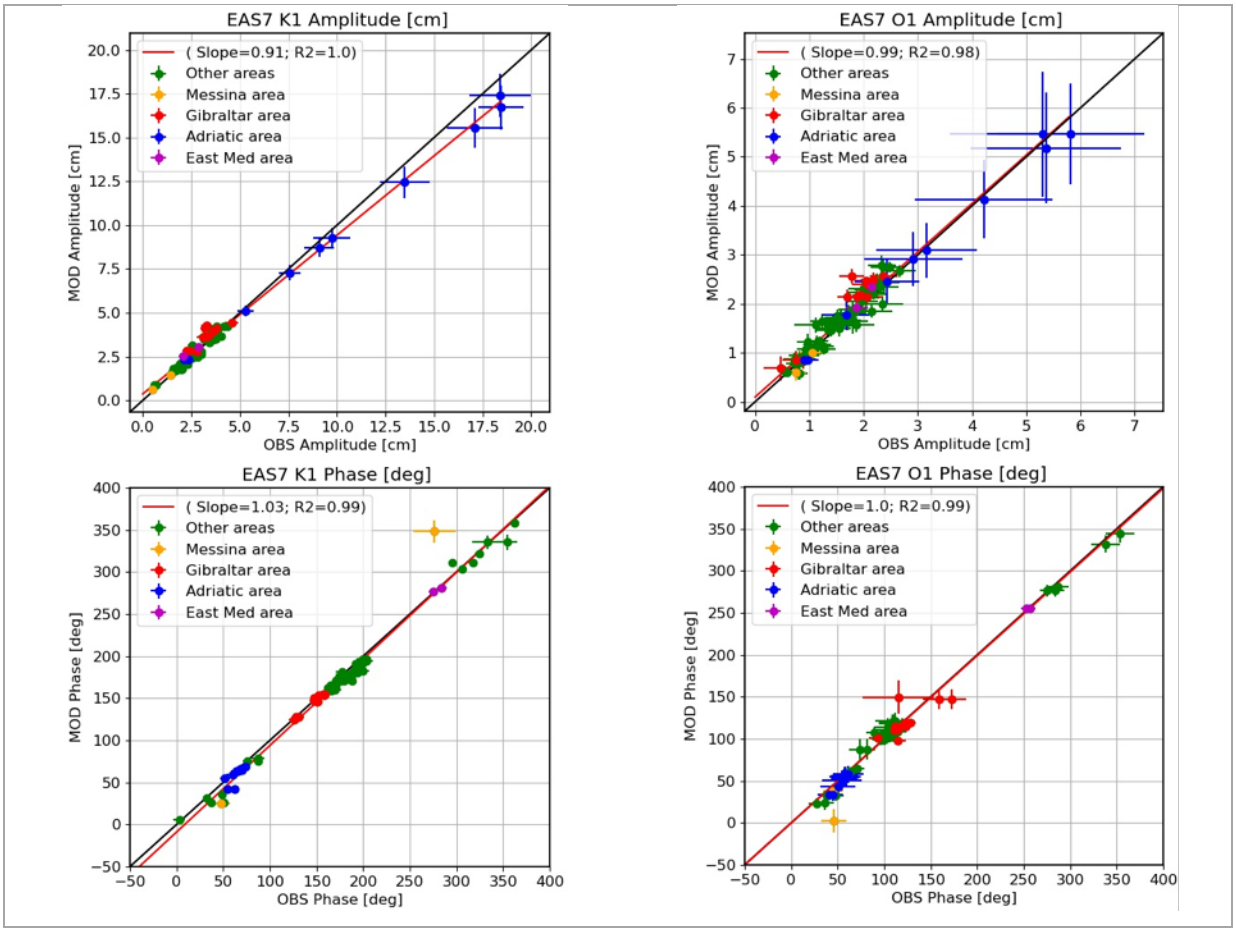

Figure 29: (continued) Scatter plot of tidal amplitude and phase for the 4 major Mediterranean Sea tidal constituents: M2, S2, K1, O1 evaluated at 98 tide gauges.

Figure 30: presents the RMS misfits evaluated from the vectorial distance for each tidal constituent, showing that the M2 component has the largest error, but it has to be considered that the amplitude of M2 tidal component is almost everywhere the greatest one.

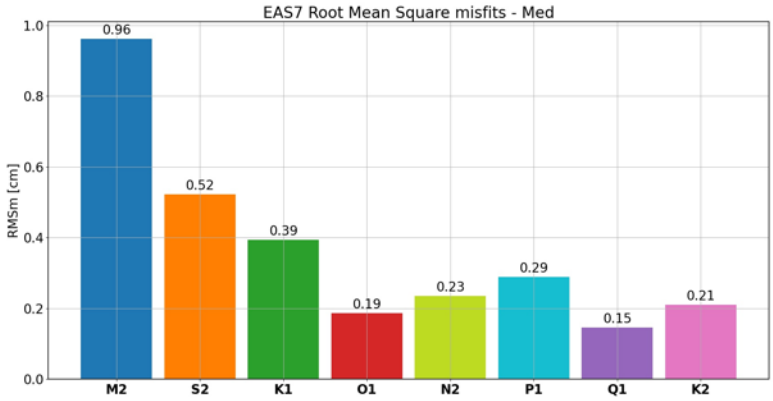

Figure 30: RMS misfits of vectorial distance between model and tide gauges tidal amplitudes for each tidal constituent

A further analysis has been performed by evaluating the vectorial distance between the model and a sub-set of 35-tide gauges (the ones in bold in Table 12) which were used in previous literature evaluations (Tsimplis et al. 1995, Palma et al. 2020). Table **13** with the mean vectorial distances evaluated for EAS7 and the ones published on reference literature is presented below, showing that EAS7 is almost always closer to observations with respect to previous studies, especially for the diurnal K1 tidal component.

Mean Vectorial distances	M2	S2	K1	O1
EAS7	1.10 cm	0.67 cm	0.59 cm	0.27 cm
Tsimplis et al., 1995	1.60 cm	0.98 cm	1.35 cm	0.41 cm
Palma et al., 2020	1.53 cm	0.86 cm	1.34 cm	0.71 cm

Table 13: Mean Vectorial distance between model and tide gauges for EAS7 system and reference literature

Finally, the EAS7 harmonic analysis results have been compared to the TPXO9 tidal barotropic model solutions and reported in the following Table 14 in terms of RMS misfits. The RMSs have been obtained including all the grid points in the Mediterranean Basin.

Tidal Component	Root Mean Square Misfits
M2	1.83 cm
S2	1.24 cm
K1	0.45 cm
O1	0.24 cm
N2	0.30 cm
P1	0.19 cm
Q1	0.09 cm
K2	0.46 cm

Table 14: RMS misfits of vectorial distance between EAS7 harmonic analysis results on the whole Mediterranean Basin and the global TPXO tidal solution

Finally, in order to analyse the tidal amplitude differences with respect to the TPXO9 model in different areas of the domain, a map of the differences has been plotted for each tidal component. In Figure 31 the amplitude differences between the EAS7 system outputs and the global barotropic TPXO9 model are shown for the first four tidal components on the whole system domain. In this Figure the red areas represent regions where EAS7 outputs overestimate the amplitude with respect to TPXO9, while the blue ones correspond to the grid points characterized by a lower amplitude with respect to TPXO9. Looking at the magnitude of the amplitude differences in Figure 31, can be stated that the EAS7 harmonic analysis results are close to the one of TPXO9 with the exception of the Gulf of Gabes where the M2 amplitude difference reaches more than 4 cm. However, should be noticed that this area is characterized by a strong tidal signal, the M2 component amplitude reaches more than 25 cm, making the relative error as small as in the other regions.

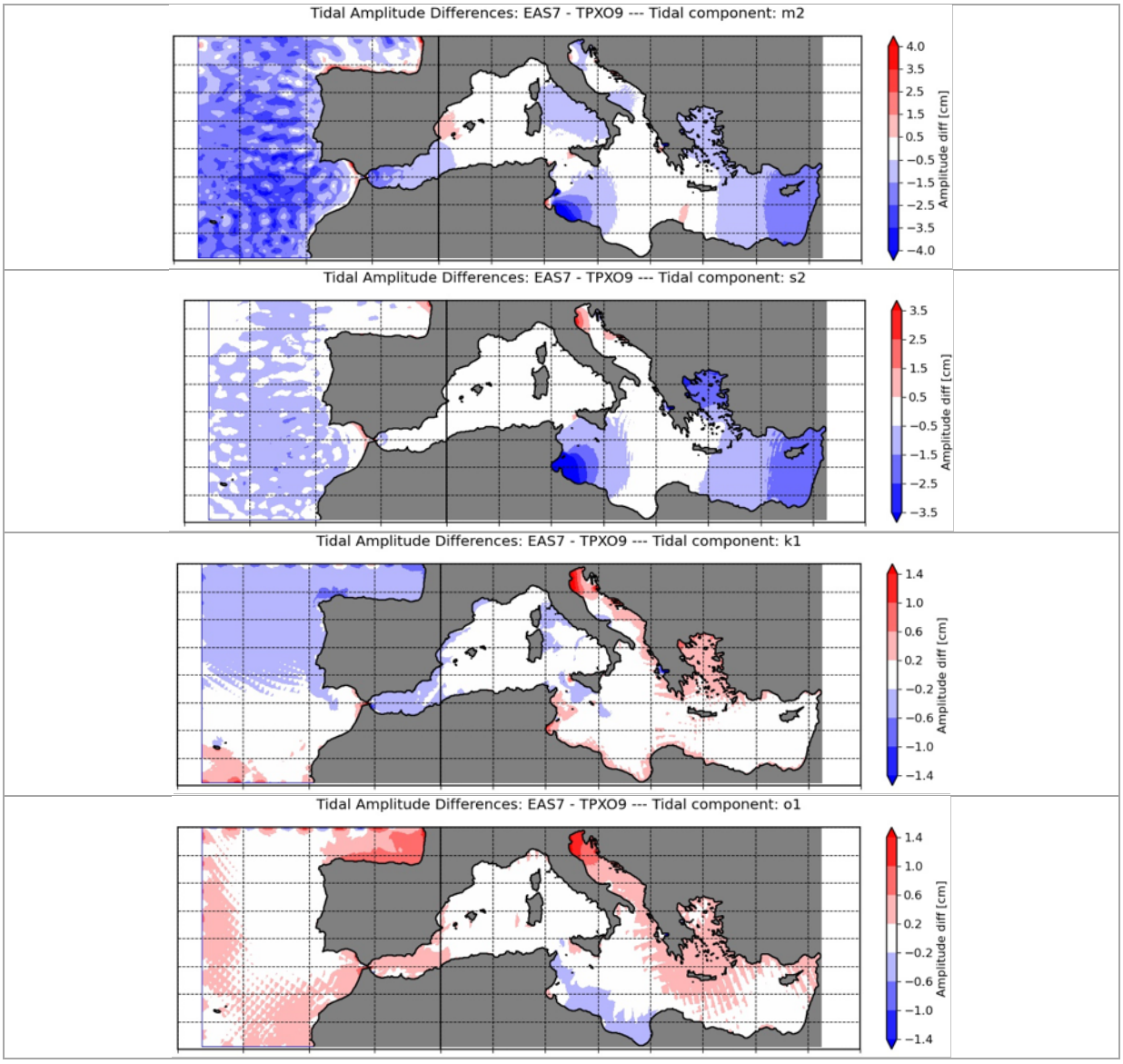

Figure 31: Tidal Amplitude differences of EAS7 with respect to TPXO9 model on the EAS7 system domain.

IV SYSTEM'S NOTICEABLE EVENTS, OUTAGES OR CHANGES

Date	Change/Event description	System version	other
8 July 2019 EIS	Updated SST nudging; Included assimilation S3B; Lateral open boundary conditions at the Dardanelles Strait.	EAS4	Time series availability: 01/01/2017 to 30 May 2020
30 March 2020 EIS	Model daily data centred at 12.00 UTC (instead 00:00 UTC).	EAS5	Time series availability: From 01/01/2018
15 Dec 2020 EIS	Upgrade of ECWMF atmospheric forcing to higher spatial and temporal resolution	EAS5	
04 May 2021 EIS	Major change of the modeling system due to inclusion of tides	EAS6	Time series availability: From 01/01/2019
29 November 2021	Time series replaced to use a corrected version of the SST satellite product (SST_MED_SST_L4_NRT_OBSERVATIONS_010_004)	EAS6	Time series availability: From 01/01/2019
14 December 2021	Use of Po river dicharge measurements instead of monthly climatologies	EAS6	Time series availability: From EIS
18 October 2022	Ingestion of Sentinel-6A SLA data	EAS6	Time series availability : From 18 October 2022
29 November 2022	Change in the modeling system due to an improved representation of tides Changes in data assimilation: use of a new Mean Dynamic Topography, assimilation of new satellites (HY-2A/B and S6) and filtered 7 km data for SLA assimilation	EAS7	Time series availability: From EIS 29 Nov 2022

V QUALITY CHANGES SINCE PREVIOUS VERSION

March 2019: From EAS4 to EAS5 system (more details in section 0).

The quality of the product is similar to the one of the previous system.

December 2020: Use of higher spatial and temporal resolution ECMWF atmospheric forcing (more details in section 0).

The quality assessment of the daily analysis physical fields carried out using the higher resolution atmospheric forcing, has provided no significantly changes with respect to the previous system.

May 2021: Inclusion of tides: the tidal potential is calculated across the domain for the 8 major constituents of the Mediterranean Sea: M2, S2, N2, K2, K1, O1, P1, Q1. In addition to this, tidal forcing is applied along the lateral boundaries in the Atlantic Ocean by means of tidal elevation and tidal currents. Reduction of the NEMO time step from 240 to 120 s. Change of model bathymetry. Increased bottom friction at Gibraltar strait. OceanVar scheme has been updated in order to account for the tidal signal in the along-track altimeter observations.

In the following figures we report the main quality changes between new system EAS6 with respect to the previous one EAS5 in terms of time averaged (year 2019) profiles of Temperature (Figure 32, Figure 33) and Salinity (Figure 34, Figure 35) RMSD and bias with respect to in-situ observations as well as daily area averaged time series of SLA with respect to satellite data (Figure 36).

In all comparison we can notice a slight decrease of both RMSD and bias in the new system EAS6 with respect to EAS5.

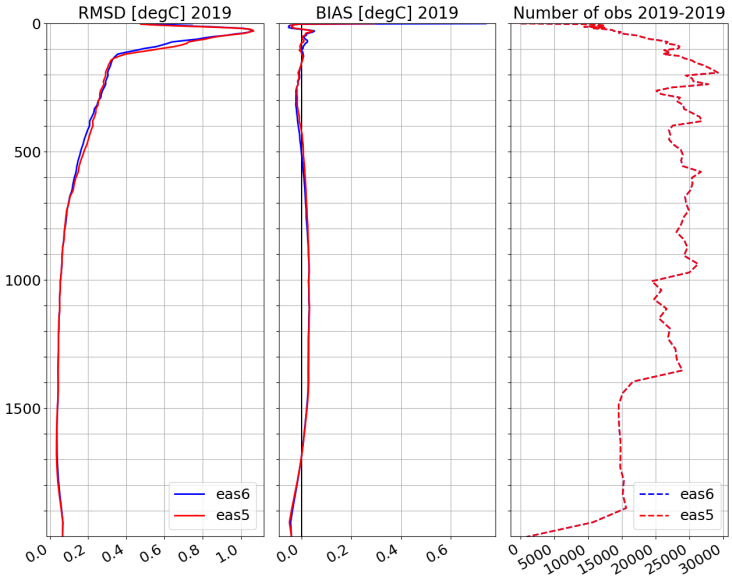

Figure 32: Time averaged (year 2019) profiles (0-2000m) of Temperature RMSD and bias with respect to in-situ observations: EAS5 (red line) and EAS6 (blue line). Right panel represent n. of observations.

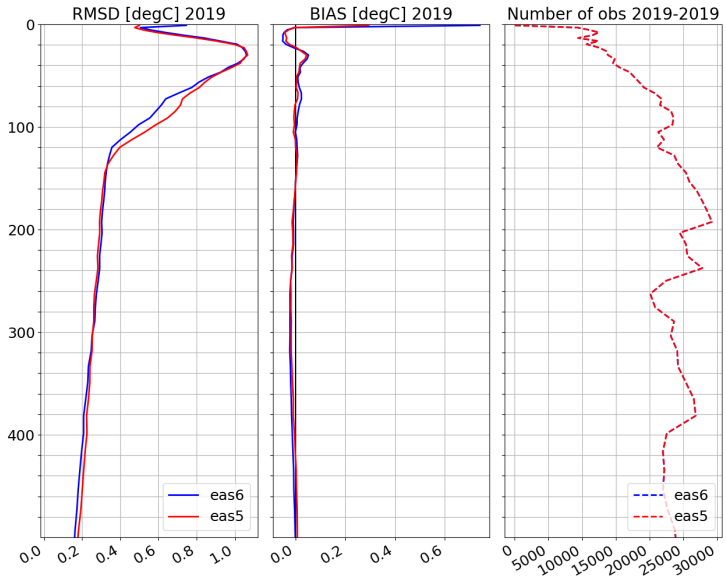

Figure 33: Time averaged (year 2019) profiles (0-500m) of Temperature RMSD and bias with respect to in-situ observations: EAS5 (red line) and EAS6 (blue line). Right panel represent n. of observations.

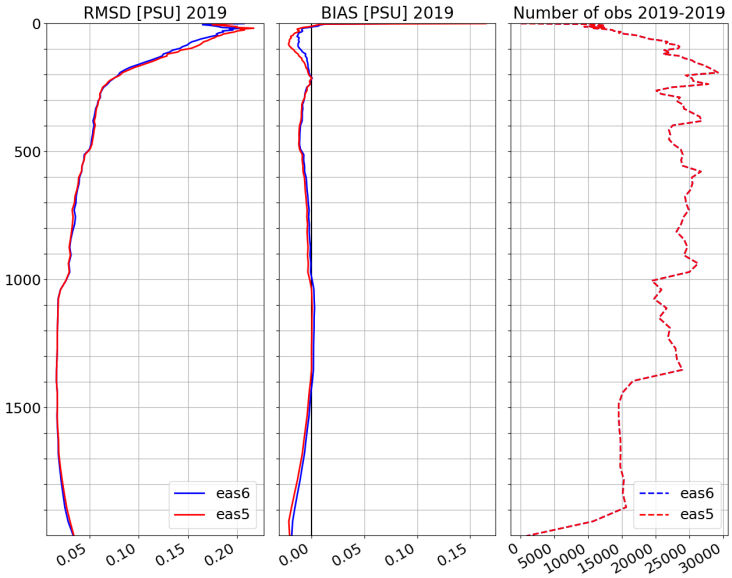

Figure 34: Time averaged (year 2019) profiles (0-2000m) of Salinity RMSD and bias with respect to in-situ observations: EAS5 (red line) and EAS6 (blue line). Right panel represent n. of observations.

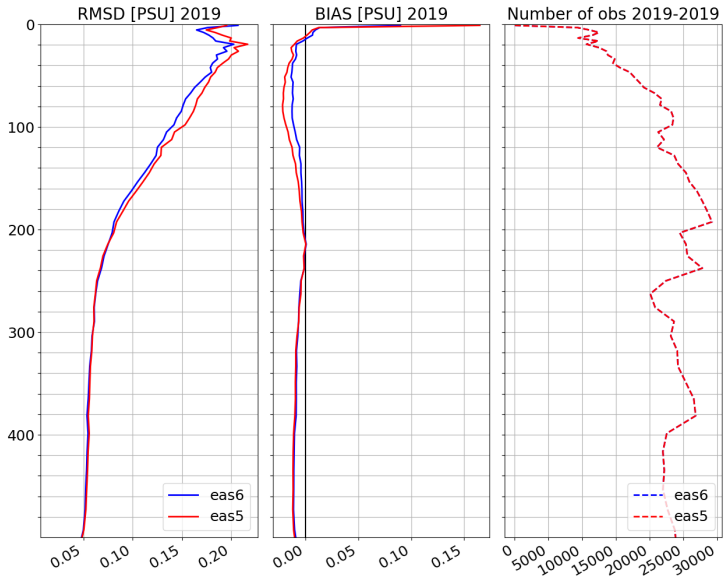

Figure 35: Time averaged (year 2019) profiles (0-500m) of Salinity RMSD and bias with respect to in-situ observations: EAS5 (red line) and EAS6 (blue line). Right panel represent n. of observations.

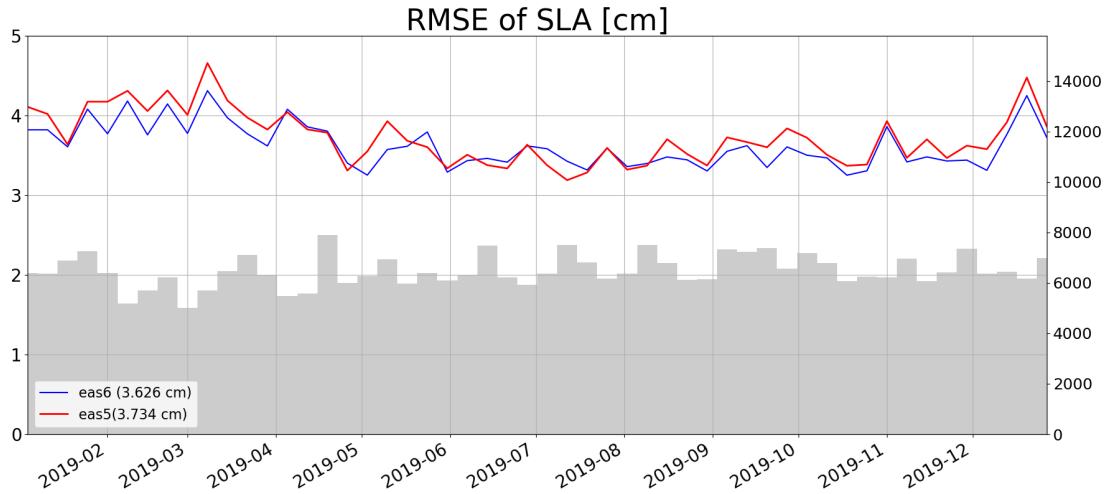

Figure 36: Time series (year 2019) of SLA RMSD with respect to satellite data: EAS5 (red line) and EAS6 (blue line). Grey bars represent n. of observations.

November 2021: Use of a corrected version of the SST L4 satellite product (SST_MED_SST_L4_NRT_OBSERVATIONS_010_004) which was affected by an issue starting from April 2019 and was replaced with a new correct dataset.

An experiment has been done in 2019 to assess the impact of the correction in the satellite SST data on the MEDSEA_ANALYSISFORECAST_PHY_006_013 product.

Figure 37 provides the SST RMSD and Bias of the new and previous model results with respect to satellite L4 data and showing that the mean impact in the whole basin is negligible.

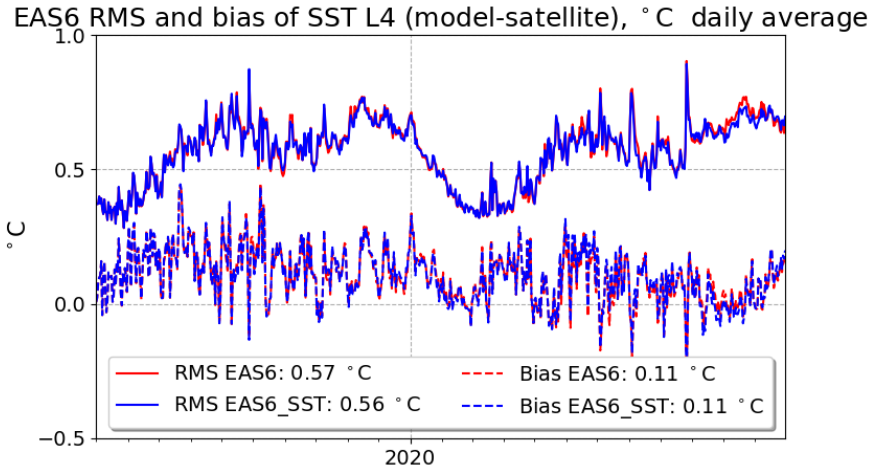

Figure 37: Time series of SST RMSD and Bias of model outputs during year 2019 compared to SST L4 satellite data for an experiment which is relaxed using corrupted data (red lines) and the new experiment using corrected SST data (blue lines).

Figure 38 provides the temperature RMSD along 9 vertical layers averaged in the whole Mediterranean Sea with respect to *insitu* observations and showing a slight decrease of the error when corrected SST data are used to relax the model non solar radiation.

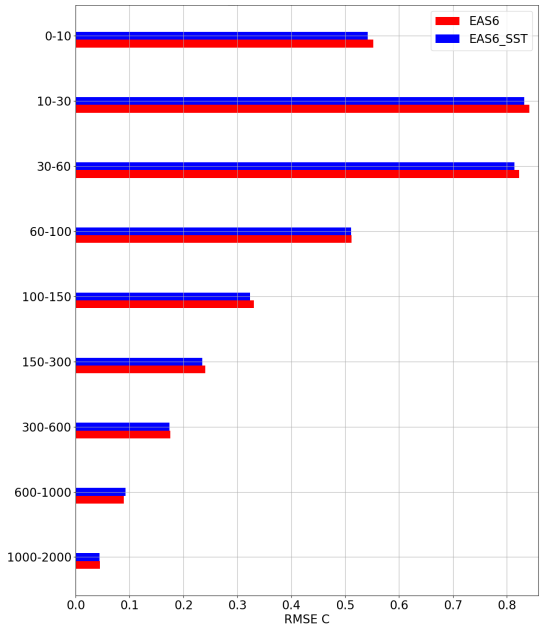

Figure 38: Temperature RMSD along 9 vertical layers: model outputs with respect to insitu observations for the experiment which is relaxed using corrupted data (red lines) and the new experiment using corrected SST data (blue lines).

December 2021: Use of daily Po river discharge measurements distributed by ARPAE (Regional Agency for Prevention, Environment and Energy of Emilia-Romagna, Italy) and available from the website: https://simc.arpae.it/dext3r/. The Po river discharge is measured at the closing point of the drainage basin in Pontelagoscuro. The measured Po river runoff is in average lower than climatological values except for several periods where large discharges were recorded (see Figure 39).

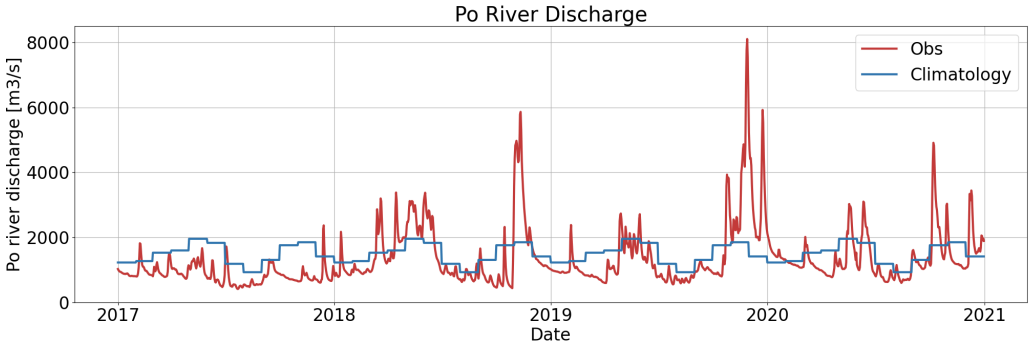

Figure 39: Time series of Po river discharge: daily measurements (red) and monthly climatologies (blue).

The model validation does not provide significant differences when considering yearly statistics in the basin and especially when data assimilation is included. Slight improvements have been achieved when comparing hindcast simulations during flooding events such as November 2018 and November-December 2019.

Figure 40 presents the RMSD (left) and Bias (right) of the model salinity evaluated in the North Adriatic Sea (region 11) during November 2018 showing that the higher frequency Po runoff produces some reduction of the salinity error especially at surface layers.

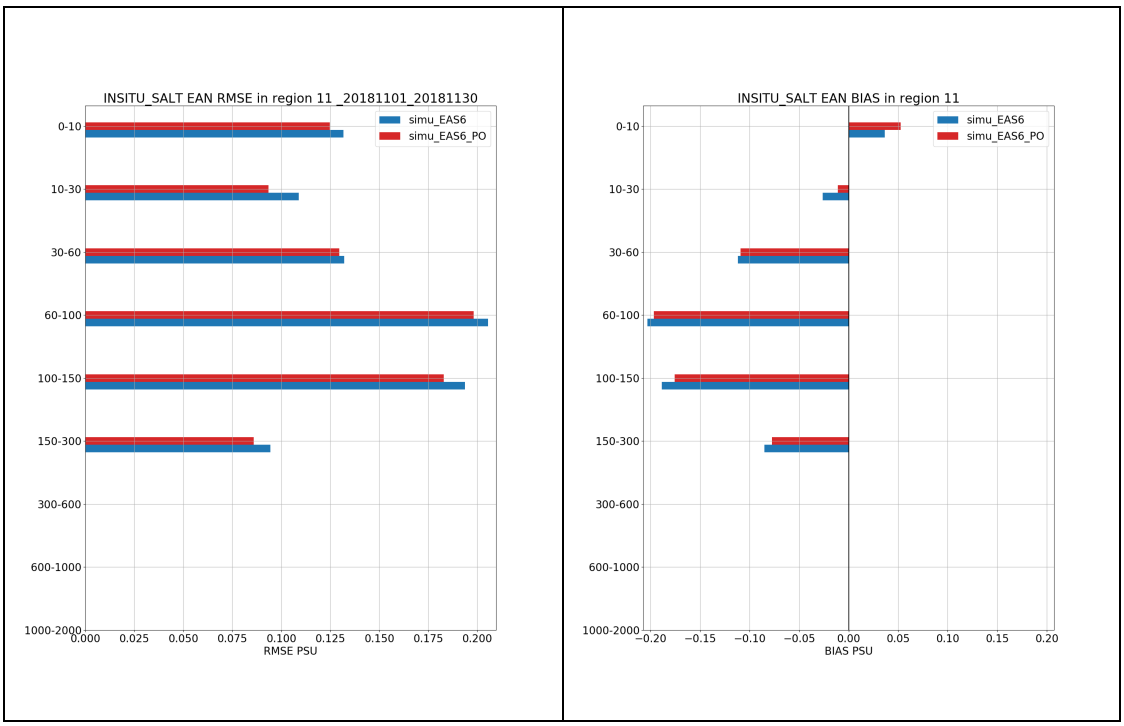

Figure 40. Salinity RMSD (left) and Bias (right) evaluated comparing the daily mean model outputs of the EAS6 experiments forced with Po river climatologies (blue) and with daily observations (red) with respect to *insitu* observations in November 2018 in the North Adriatic Sea (region 11).

Similar results are achieved in the period November-December 2019 (period of large Po river discharge) and presented in Figure 41.

However we should consider that a validation analysis in such a short period and in this small and shallow area is affected by the low availability of *insitu* data.

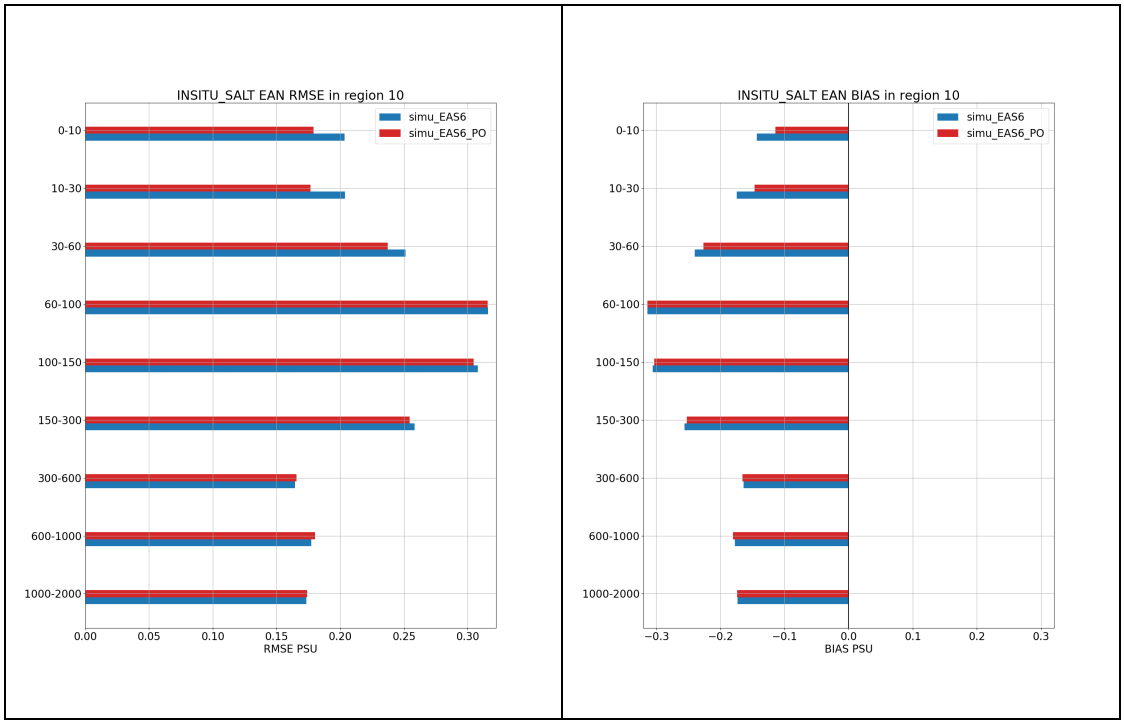

Figure 41. Salinity RMSD (left) and Bias (right) evaluated comparing the daily mean model outputs of the EAS6 experiments forced with Po river climatologies (blue) and with daily observations (red) with respect to insitu observations in November-December 2019 in the South Adriatic Sea (region 10).

October 2022: Ingestion of Sentinel-6A (S6A) Sea Level Anomaly Satellite Altimeter Observations.

The impact of the assimilation of SLA data in the EAS6 system is investigated for the period 28 March - 28 June 2022 (in total three months). The operational system EAS6 has been run with and without the ingestion of SLA observations from S6A, namely EAS6_mfs1_s6a and EAS6_mfs1_nos6a, respectively.

In the following Table 15 the mean RMS misfits (known also as innovations) calculated at observation time during the forward model integration (called first guess at appropriate time or FGAT) are provided for SLA, temperature (T) and salinity (S), at different model layers for temperature and salinity (1-15 m, 15-45 m, 45-135 m, 100-200 m, 200-400 m, 400-800 m).

	No Sentinel-6A (EAS6_mfs1_nos6a)		**Sentinel-6A (EAS6_mfs1_s6a)**	
SLA (cm)	3.1		3.0	
	T (°C)	**S (psu)**	**T (°C)**	**S (psu)**

1-15 m	0.65	0.18	0.67	0.17
15-45 m	0.63	0.16	0.61	0.15
45 - 135 m	0.30	0.12	0.30	0.12
100-200 m	0.22	0.083	0.23	0.085
200 - 400 m	0.20	0.048	0.20	0.049
400 - 800 m	0.11	0.028	0.12	0.029

Table 15: Time and space averaged RMS misfits of SLA with respect to all available satellites and of Temperature and Salinity along 6 vertical layers for the twin experiment with (EAS6_mfs1_s6a) and without (EAS6_mfs1_s6a) assimilation of Sentinel-6A SLA observations.

Figure 43: Comparison between the scatter plots of M2 tidal component amplitude and phase with respect to tide-gauge data obtained from the harmonic analysis applied to the EAS6 and EAS7 versions.Figure 43 presents the RMS of SLA misfits between 28 March 2022 and 28 June 2022 for the twin experiments showing a reduced misfit when S6A SLA observations are assimilated. The error evolution of the experiments is close in the first days, since they start from the same initial conditions, while after 2 weeks the assimilation of S6A data produces a reduction of the RMS misfits from 3.1 cm to 3 cm. We note that the amount of data ingested has increased by approximately 20% with the introduction of S6A.

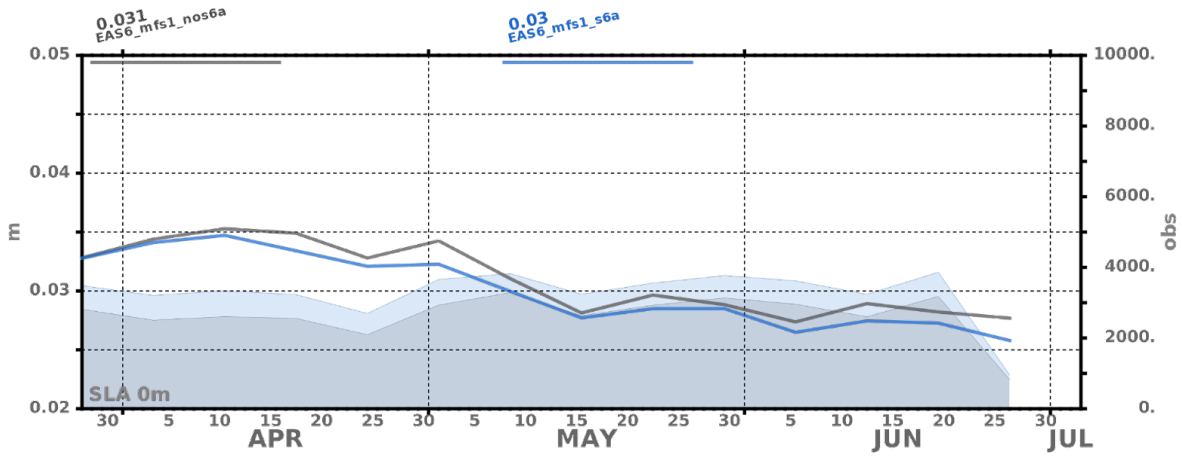

Figure 42: Weekly time series of RMS of SLA misfits between 28 March 2022 and 28 June 2022. The experiment EAS6_mfs1_nos6a without Sentinel-6A assimilation (grey line) and EAS6_mfs1_s6a with Sentinel-6A assimilation (blue) are shown. The time averaged RMS of SLA misfits (m) is printed on the legend. The number of assimilated observations (right y-axis) is shaded with the respective colour.

The analysis shows that the information incorporated with the new dataset is in agreement with the already existing ones and does not degrade the system. There are some improvements at the sampling locations of other satellites as demonstrated by the misfit statistics. The temperature and salinity estimates are also evaluated since they are directly updated by SLA assimilation. First findings reveal differences in temperature and salinity with close error estimates.

November 2022: The representation of tides has been improved including a Topographic Wave Drag parameterization and a correction to the Bottom Friction coefficient. In Table 16 and Table 17 the improvements on the model output, with respect to the previous model version, are shown in terms of salinity and temperature misfits over the five-years period 2017-2021. For what concerns the temperature, the comparison does not provide significant differences while, for salinity, a slight improvement can be noticed.

System version	S [PSU] 8 m	S [PSU] 30 m	S [PSU] 150 m	S [PSU] 300 m	S [PSU] 600 m
EAS7	0.17±0.03	0.16±0.04	0.09±0.02	0.047±0.008	0.029±0.005
EAS6	0.17±0.03	0.17±0.03	0.10±0.02	0.048±0.004	0.029±0.005

Table 16: Comparison between salinity RMSD misfits obtained from EAS7 and EAS6 system versions with respect to insitu observations. The values have been computed on the period 2017-2021

System version	T [°C] 8 m	T [°C] 30 m	T [°C] 150 m	T [°C] 300 m	T [°C] 600 m
EAS7	0.56±0.20	0.78±0.42	0.25±0.06	0.18±0.04	0.11±0.02
EAS6	0.54±0.20	0.78±0.44	0.26±0.06	0.19±0.04	0.11±0.02

Table 17: Comparison between temperature RMSD misfits obtained from EAS7 and EAS6 system versions with respect to insitu observations. The values have been computed on the period 2017-2021

Moreover Gibraltar and Messina Straits parameterizations have been modified. In particular the increased bottom friction in the area outside Gibraltar strait has been removed while the lateral friction inside the strait has been doubled. The gain due to this modification, that contributes to the improvements shown in Table 16, concerns the salinity.

For what concerns the Messina strait, the area of enhanced lateral friction has been modified. Comparing the tidal phase obtained from harmonic analysis applied to the EAS6 and EAS7 system versions, clear improvements appear. See Figure 43 where the comparison between the scatter plots for amplitude and phase of the main tidal component, namely M2, are compared between the two system version. The points concerning the Messina area are the orange ones. General improvements in the harmonic analysis results can be stated also looking at the Slope and R2 parameters obtained from the linear regression given in the legends of the plots in Figure 43.

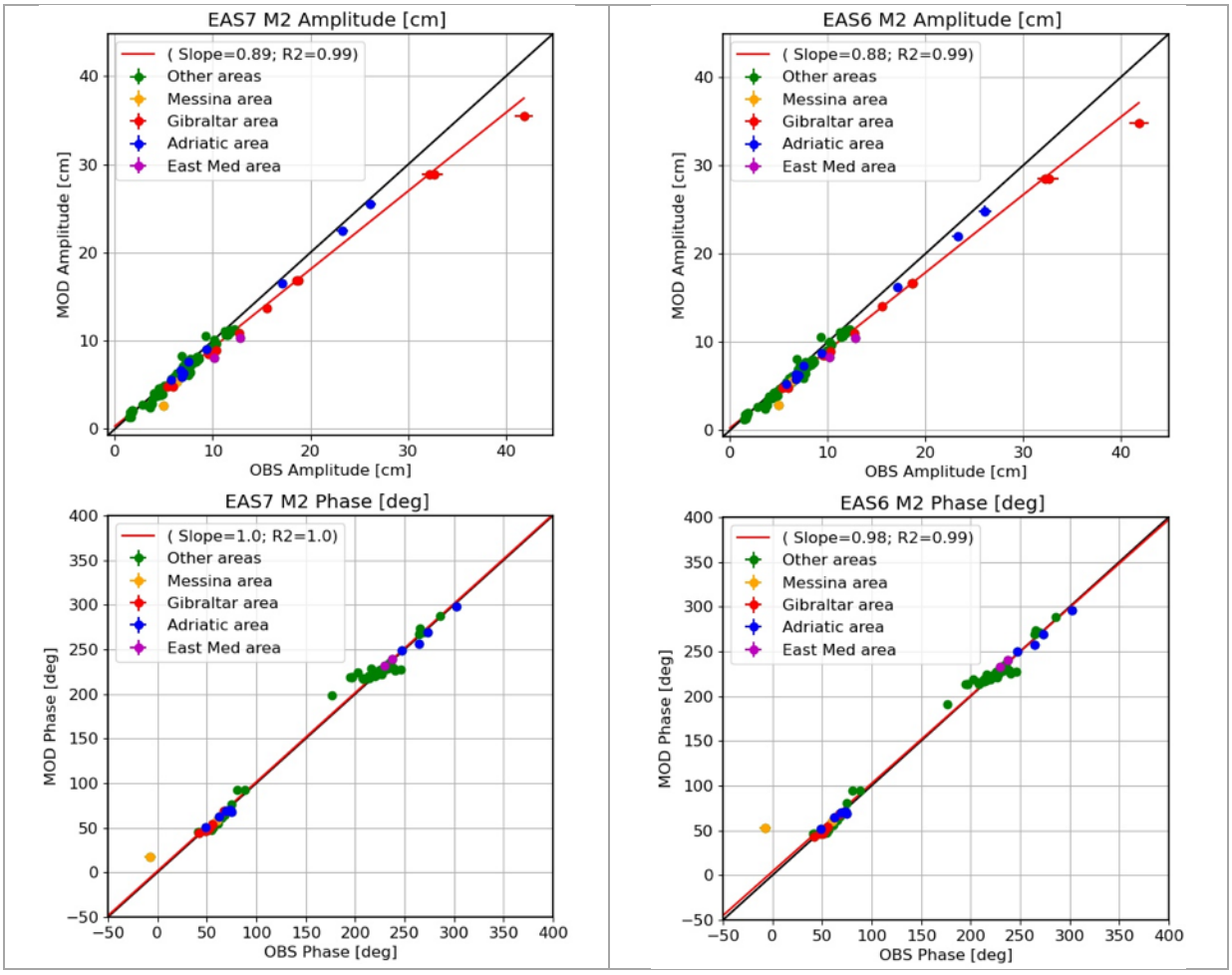

Figure 43: Comparison between the scatter plots of M2 tidal component amplitude and phase with respect to tide-gauge data obtained from the harmonic analysis applied to the EAS6 and EAS7 versions.

Finally the use of a new MDT, filtered 7 km data and new satellite data (HY-2A/B and S6) for SLA assimilation have shown to provide a major improvement in RMSD of SLA, see Figure 44 where the comparison with respect to the previous system is depicted in terms of SLA RMSD of misfits obtained on a five-year period 2017-2021. The mean value over the whole period moves from 3.36±0.24 cm to 3.04±0.24 cm.

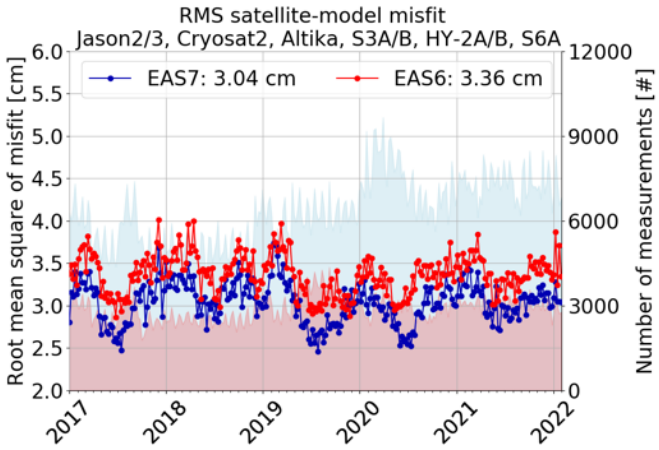

Figure 44: Comparison between SLA RMSD misfits obtained from EAS7 and EAS6 system versions with respect to satellite data. The values have been computed on the period 2017-2021

VI REFERENCES

Borile F.: Towards a broader understanding of the effects of tidal forcing on the global ocean circulation (PhD thesys, 2022)

Carrere L., F. Lyard, M. Cancet, A. Guillot, N. Picot: FES 2014, a new tidal model – Validation results and perspectives for improvements, presentation to ESA Living Planet Conference, Prague 2016.

Clementi, E., Pistoia, J., Delrosso, D., Mattia, G., Fratianni, C., Storto, A., Ciliberti, S., Lemieux, B., Fenu, E., Simoncelli, S., Drudi, M., Grandi, A., Padeletti, D., Di Pietro, P., Pinardi, N., (2017a). A 1/24 degree resolution Mediterranean analysis and forecast modelling system for the Copernicus Marine Environment Monitoring Service. Extended abstract to the 8th EuroGOOS Conference, Bergen.

Clementi, E., Oddo, P., Drudi, M., Pinardi, N., Korres, G., Grandi A., (2017b). Coupling hydrodynamic and wave models: first step and sensitivity experiments in the Mediterranean Sea. *Ocean Dynamics*. doi: https://doi.org/10.1007/s10236-017-1087-7.

Desroziers, G., Berre, L., Chapnik, B. and Poli, P., (2005). Diagnosis of observation, background and analysis-error statistics in observation space. Q.J.R. Meteorol. Soc. 131: 3385–3396. doi: 10.1256/qj.05.108.

Dobricic Srdjan, and Nadia Pinardi (2008). An oceanographic three-dimensional variational data ssimilation scheme. Ocean Modelling, 22 (3-4) 89-105.

Dobricic, S., Pinardi, N., Adani, M., Tonani, M., Fratianni, C., Bonazzi, A., Fernandez, V., (2007). Daily oceanographic analyses by Mediterranean Forecasting System at the basin scale. Ocean Sci., 3, 149-157.

Dobricic, Srdjan (2005). New mean dynamic topography of the mediterranean calculated fron assimilation system diagnostic. GRL, 32.

Dombrowsky, E., Bertino, L., Brassington, G.B., Chassignet, E.P., Davidson, F., Hurlburt, H.E., Kamachi, M., Lee, T., Martin, M.J., Meu, S., Tonani M., (2009). GODAE Systems in operation, Oceanography, Volume 22-3, 83,95.

Drevillon, M., Bourdalle-Badie, R., Derval, C., Drillet, Y., Lelouche, J. M., Remy, E., Tranchant, B., Benkiran, M., Greiner, E., Guinehut, S., Verbrugge, N., Garric, G., Testut, C. E., Laborie, M., Nouel, L., Bahurel, P., Bricaud, C., Crosnier, L., Dombrosky, E., Durand, E., Ferry, N., Hernandez, F., Le Galloudec, O., Messal, F., Parent, L. (2008). The GODAE/MercatorOcean global ocean forecasting system: results, applications and prospects, J. Operational Oceanogr., 1(1), 51–57.

Estubier A., and Levy M., (2000). Quel schema numerique pour le transport d'organismes biologiques par la circulation oceanique. Note Techniques du Pole de modelisation, Institut Pierre-Simon Laplace, pp 81

Fekete, B. M., Vorosmarty, C. J., Grabs, W., (1999). Global, Composite Runoff Fields Based on Observed River Discharge and Simulated Water Balances, Tech. Rep. 22, Global Runoff Data Cent., Koblenz, Germany.

Flather, R.A. (1976). A tidal model of the northwest European continental shelf. Memories de la Societe Royale des Sciences de Liege 6 (10), 141–164

Gunther, H., Hasselmann, H., Janssen, P.A.E.M., (1993). The WAM model cycle 4, DKRZ report n. 4.

Hasselmann, K. (1974). On the characterization of ocean waves due to white capping, Boundary-Layer Meteorology, 6, 107-127.

Hasselmann, S., and Hasselmann, K. (1985). Computations and parameterizations of the nonlinear energy transfer in a gravity wave spectrum. Part I: A new method for efficient computations of the exact nonlinear transfer integral, J. Phys. Ocean., 15, 1369-1377.

Hasselmann, S., Hasselmann, K., Allender, J.H., Barnett, T.P., (1985). Computations and parameterizations of the nonlinear energy transfer in a gravity wave spectrum. Part II: Parameterizations of the nonlinear energy transfer for application in wave models, J. Phys. Ocean., 15, 1378-1391.

Houpert, L., Testor, P., Durrieu De Madron, X., (2015). Gridded climatology of the Mixed Layer (Depth and Temperature), the bottom of the Seasonal Thermocline (Depth and Temperature), and the upper-ocean Heat Storage Rate for the Mediterrean Sea. SEANOE. http://doi.org/10.17882/46532

Janssen, P.A.E.M. (1989). Wave induced stress and the drag of air flow over sea wave, J. Phys. Ocean., 19, 745-754.

Janssen, P.A.E.M. (1991). Quasi-Linear theory of wind wave generation applied to wave forecasting, J. Phys. Ocean., 21, 1631-1642.

Komen, G.J., Hasselmann, S., Hasselmann, K., (1984). On the existence of a fully developed windsea spectrum, J. Phys. Ocean., 14, 1271-1285.

Kourafalou, V.H., and Barbopoulos, K., (2003). High resolution simulations on the North Aegean Sea seasonal circulation, Ann. Geophys., 21, 251–265.

Lynch, D.R and W.G. Gray (1979). A wave equation model for finite element tidal computations. In: Computers & fluids 7.3, pp. 207–228.

Maraldi C., Chanut, J., Levier, B., Ayoub, N., De Mey, P., Reffray, G., Lyard, F., Cailleau, S., Drévillon, M., Fanjul, E.A., Sotillo, M.G., Marsaleix, P., and the Mercator Research and Development Team (2013). NEMO on the shelf: assessment of the Iberia–Biscay–Ireland configuration. Ocean Sci., 9, 745–771.

Madec, G. and the NEMO system Team. NEMO Ocean Engine, Scientific Notes of Climate Modelling Center (27) - ISSN 1288-1619, Institut Pierre-Simon Laplace (IPSL) 2019, http://doi.org/10.5281/zenodo.1464816.

Maderich V., Ilyin Y., Lemeshko E., 2015. Seasonal and interannual variability of the water exchange in the Turkish Straits System estimated by modelling. Mediterranean Marine Science, [S.l.], v. 16, n. 2, p. 444-459, ISSN 1791-6763, doi:http://dx.doi.org/10.12681/mms.1103.

Marchesiello, P., McWilliams, J. C., Shchepetkin, A., (2001). Open boundary conditions for long-term integration of regional oceanic models. Ocean modelling, 3(1), 1-20.

Oddo, P., Adani, M., Pinardi, N., Fratianni, C., Tonani, M., Pettenuzzo, D., (2009). A Nested Atlantic-Mediterranean Sea General Circulation Model for Operational Forecasting. Ocean Sci. Discuss., 6, 1093-1127.

Oddo, P., Bonaduce, A., Pinardi, N., Guarnieri, A., (2014) Sensitivity of the Mediterranean sea level to atmospheric pressure and free surface elevation numerical formulation in NEMO. Geosci. Model Dev., 7, 3001–3015.

Palma M.et al. (2020). Short-term, linear, and non-linear local effects of the tides on the surface dynamics in a new, high-resolution model of the Mediterranean Sea circulation. Ocean Dynamics, 70. DOI: 10.1007/s10236-020-01364-6

Pinardi, N., Allen, I., De Mey, P., Korres, G., Lascaratos, A., Le Traon, P.Y., Maillard, C., Manzella G., Tziavos, C., (2003). The Mediterranean ocean Forecasting System: first phase of implementation (1998-2001). Ann. Geophys., 21, 1, 3-20.

Pistoia, J., Clementi, E., Delrosso, D., Mattia, G., Fratianni, C., Drudi, M., Grandi, A., Padeletti, D., Di Pietro, P., Storto, A., Pinardi., N., (2017). Last improvements in the data assimilation scheme for the Mediterranean Analysis and Forecast system of the Copernicus Marine Service. Extended abstract to the 8th EuroGOOS Conference, Bergen.

Pacanowsky, R.C., and Philander S.G.H., (1981) Parameterization of vertical mixing in numerical models of tropical oceans. J Phys Oceanogr 11:1443-1451

Pettenuzzo, D., Large, W.G., Pinardi, N., (2010) On the corrections of ERA-40 surface flux products consistent with the Mediterranean heat and water budgets and the connection between basin surface total heat flux and NAO. Journal of Geophysical Research 115, C06022, doi:10.1029/2009JC005631

Provini, A., Crosa, G., Marchetti, R., (1992). Nutrient export from Po and Adige river basins over the last 20 years. Sci. Total Environ; suppl.: 291-313

Raicich, F. (1996). On fresh water balance of the Adriatic Sea, J. Mar. Syst., 9, 305–319.

Rio, M.-H., Pascual, A., Poulain, P.-M., Menna, M., Barceló, B., Tintoré, J., (2014). Computation of a new mean dynamic topography for the Mediterranean Sea from model outputs, altimeter measurements and oceanographic in situ data. Ocean Science, 10, 731-744.

Roullet, G., and Madec G., (2000). Salt conservation, free surface, and varying levels: a new formulation for ocean general circulation models. J.G.R., 105, C10, 23,927-23,942.

Shakespeare, C. J., Arbic, B. K., and Hogg, A. M. (2020). The drag on the barotropic tide due to the generation of baroclinic motion. Journal of Physical Oceanography, 50:3467–3481.

Soto-Navaro, J., Criado-Aldeanueva, F., Garci-Lafuente, J., Sanchez-Roman, A., (2010). Estimation of the Atlantic inflow through the Strait of Gibraltar from climatological and in situ data. J. Jeophysics Research, 10.1029/2010JC006302

Storto, A., Masina, S., Navarra, A., (2015). Evaluation of the CMCC eddy-permitting global ocean physical reanalysis system (C-GLORS, 1982-2012) and its assimilation components. *Quarterly Journal of the Royal Meteorological Society*, 142, 738–758, doi: 10.1002/qj.2673.

Tolman H.L. (2009). User Manual and system documentation of WAVEWATCH III version 3.14. NOAA/NWS/NCEP/MMAB Technical Note 276, 194 pp + Appendices.

Tolman H.L. (2002). Validation of WAVEWATCH III version 1.15 for a global domain.NOAA / NWS / NCEP / OMB Technical Note 213, 33 pp.

Tonani, M., Balmaseda, M., Bertino, L., Blockley, E., Brassington, G., Davidson, F., Drillet, Y., Hogan, P., Kuragano, T., Lee, T., Mehra, A., Paranathara, F., Tanajura, CAS, Wang, H., (2015) Status and future of global and regional ocean prediction systems. J Operational Oceanography 8:201-220, doi:10.1080/1755876X.2015.1049892.

Tonani, M., Teruzzi, A., Korres, G., Pinardi, N., Crise, A., Adani, M., Oddo, P., Dobricic, S., Fratianni, C., Drudi, M., Salon, S., Grandi, A., Girardi, G., Lyubartsev, V., Marino, S., (2014). The Mediterranean Monitoring and Forecasting Centre, a component of the MyOcean system. Proceedings of the 6th Int. Conference on EuroGOOS 4-6 October 2011, Sopot, Poland. Edited by H. Dahlin, N.C. Fleming and S. E. Petersson. First published 2014. Eurogoos Publication no. 30. ISBN 978-91-974828-9-9.

Tonani, M., Pinardi, N., Dobricic, S., Pujol, I., Fratianni, C., (2008). A high-resolution free-surface model of the Mediterranean Sea. Ocean Sci., 4, 1-14.

Tonani, M., Simoncelli, S., Grandi, A., Pinardi, N., (2013). New gridded climatologies, from in-situ observations, for the Mediterranean Sea. Abstract to IMDIS 2013.

https://imdis.seadatanet.org/content/download/93851/1140805/file/SDN2_D64_WP6_IMDIS2013_proceedings_abstracts.pdf

Tsimplis, M.N., Proctor, R., Flather, R. A. (1995). Two-dimensional tidal model for the Mediterranean Sea. J. of Geophysical Research. https://doi.org/10.1029/95JC01671

Van Leer, B. (1979) Towards the Ultimate Conservative Difference Scheme, V. A Second Order Sequel to Godunov's Method. J Comp Phys 32:101-136